

[Click here to view linked References](#)

1 **Draft genome of the honey bee ectoparasitic mite, *Tropilaelaps mercedesae*, is shaped by the**
2 **parasitic life history**

33
44
55
65 Xiaofeng Dong¹, Dong Xia², Stuart D Armstrong², Benjamin L. Makepeace², Alistair C. Darby³, and
76 Tatsuhiko Kadowaki^{1*}

87
97
108
119 ¹Department of Biological Sciences, Xi'an Jiaotong-Liverpool University, 111 Ren'ai Road, Suzhou
120 Dushu Lake Higher Education Town, Jiangsu Province 215123, China

141 ²Institute of Infection & Global Health, University of Liverpool, Liverpool L3 5RF, United Kingdom

162 ³Institute of Integrative Biology, University of Liverpool, Liverpool L69 7ZB, United Kingdom

173
184
194 Corresponding author:

205 Tatsuhiko Kadowaki

216 Department of Biological Sciences, Xi'an Jiaotong-Liverpool University

217 111 Ren'ai Road, Suzhou Dushu Lake Higher Education Town

248 Jiangsu Province 215123, China

269 TEL: 86 512 88161659, FAX: 86 512 88161899

270 E-mail: Tatsuhiko.Kadowaki@xjtlu.edu.cn

281
292 E-mail addresses of authors:

313 Xiaofeng Dong: Xiaofeng.dong12@student.xjtlu.edu.cn

324 Dong Xia: dongxia@liverpool.ac.uk

345 Stuart D Armstrong: sarmstro@liverpool.ac.uk

366 Benjamin L. Makepeace: blm1@liverpool.ac.uk

377 Alistair C. Darby: Alistair.Darby@liverpool.ac.uk

31 **Abstract**

32 **Background**

33 The number of managed honey bee colonies has considerably decreased in many developed
34 countries in recent years and ectoparasitic mites are considered as major threats to honey bee
35 colonies and health. However, their general biology remains poorly understood.

36 **Results**

37 We sequenced the genome of *Tropilaelaps mercedesae*, the prevalent ectoparasitic mite infesting
38 honey bees in Asia and predicted 15,190 protein-coding genes which were well supported by the
39 mite transcriptomes and proteomic data. Although amino acid substitutions have been accelerated
40 within the conserved core genes of two mites, *T. mercedesae* and *Metaseiulus occidentalis*, *T.*
41 *mercedesae* has undergone the least gene family expansion and contraction between the seven
42 arthropods we tested. The number of sensory system genes has been dramatically reduced but *T.*
43 *mercedesae* contains all gene sets required to detoxify xenobiotics. *T. mercedesae* is closely
44 associated with a symbiotic bacterium (*Rickettsiella grylli*-like) and DWV, the most prevalent honey
45 bee virus.

46 **Conclusions**

47 *T. mercedesae* has a very specialized life history and habitat as the ectoparasitic mite strictly depends
48 on the honey bee inside a stable colony. Thus, comparison of the genome and transcriptome
49 sequences with those of a tick and free-living mites has revealed the specific features of the genome
50 shaped by interaction with the honey bee and colony environment. Genome and transcriptome
51 sequences of *T. mercedesae*, as well as *Varroa destructor*, not only provide insights into the mite
52 biology, but may also help to develop measures to control the most serious pests of the honey bee.

53
54 **Keywords:** Honey bee decline, Honey bee ectoparasitic mite, Genome, Transcriptome, Proteome,
55 Comparative genomics, Host-Parasite interaction
56

57 **Background**

58 The number of managed honey bee (*Apis mellifera*) colonies has considerably decreased in many
59 developed countries in recent years [1]. Although there are many potential causes for the decline,
60 pathogens and parasites of the honey bee, particularly ectoparasitic mites, are considered major
61 threats to honey bee colonies and health [2]. *Varroa destructor* is present globally and causes
62 abnormal brood development and brood death in honey bees, and is also responsible for the spread of
63 honey bee pathogens and parasites [3]. *Tropilaelaps mercedesae* (small honey bee mite) is another
64 honey bee ectoparasitic mite which is prevalent in most Asian countries [4]. Thus, these two mite
65 species usually co-exist in a honey bee colony in Asia, and the negative impacts of *T. mercedesae*
66 infestation on honey bees are principally the same as those of *V. destructor*, except that *T.*
67 *mercedesae* cannot feed on adult honey bees [4]. The original host of *T. mercedesae* is the giant
68 Asian honey bee, *Apis dorsata*, and like *V. destructor*, it shifted hosts to infest *A. mellifera* when
69 these colonies were brought into Asia [4]. Although *T. mercedesae* is currently restricted to Asia, it
70 has the potential to spread and establish all over the world due to the global trade of honey bees. This
71 is exactly what happened with *V. destructor* [5].

72 *V. destructor* and *T. mercedesae* are major threats to the current apiculture industry; however, we
73 still do not completely understand their sensory system, development, sex
74 determination/differentiation, reproduction, and the capability to acquire miticide (for example,
75 tau-fluvalinate and flumethrin) resistance. Genomic features of *V. destructor* was briefly reported
76 before and the associated bacteria and viruses were identified [6]. In this study, we sequenced the
77 genome and transcriptomes of *T. mercedesae*, supplemented by proteomic data, to provide insights
78 into the above aspects and understand how the mite has evolved under a very specialized
79 environment - inside the honey bee colony by depending on the honey bee as the sole host. We will
80 discuss how *T. mercedesae* may have adapted to its host and environment by shaping its genome.

82 **Results and Discussion**

83 **Genome assembly, repeated sequences, and gene annotation**

84 Each of dual indexed paired-end DNA library was prepared from a single adult male and female *T.*
85 *mercedesae* for whole-genome sequencing using the Illumina shotgun platform (Supplementary
86 Table 1). The “cleaned” reads from the male mite were then re-assembled into 34,155 scaffolds with
87 an N50 of 28,807 bp representing ~353 Mb of genomic sequence, from which we predicted 15,190
88 protein-coding genes (Table 1 and Supplementary Table 2). We found that 94.1% of the sequence
89 reads could be mapped back to this assembly and 244 (98.4%) out of the 248 Conserved Eukaryotic
90 Genes [7] as well as 83% of 2,675 arthropod BUSCOs [8] were annotated from the assembled
91 genome (Supplementary Table 3). These are comparable to those reported for nine other arachnids
92 (Table 1 and Supplementary Table 3). Proteomic characterization of the adult males and females
93 yielded 124,798 mass spectra in total and 60,463 were assigned to the peptides of annotated proteins
94 above (Supplementary file 1). With k-mer statistics [9], the size of the *T. mercedesae* genome was
95 estimated to be 660 Mb with a peak sequencing depth of ~60X, and thus approximately 50% of the
96 genome DNA was inferred to comprise repetitive sequences (Supplementary Fig. 1). Repetitive
97 sequences such as DNA transposons, retrotransposons including LINE (Long Interspersed Nuclear
98 Element), SINE (Short Interspersed Nuclear Element), and LTR (Long Terminal Repeat) as well as

99 satellite DNA represent only 7 % of the assembly (Supplementary Table 4) but the majority of them
100 were found in the high-coverage regions of the genome (Supplementary Table 5) suggesting that
101 repetitive sequences have been collapsed in the genome assembly. We thus concluded that the
102 qualities of draft genome sequence and protein-coding gene set were sufficiently robust for further
103 characterization of *T. mercedesae* genome and transcriptome.

104 Flow cytometric measurement of *T. mercedesae* nuclear DNA content together with the k-mer
105 statistics demonstrated that the male mite assumed to be haploid with ~660 Mb (1C) DNA. The
106 female mite was twice that size and assumed to be diploid at 1,287 Mb (2C) DNA (Supplementary
107 Fig. 2). Thus, *T. mercedesae* may use haplodiploidy for sex determination, and the genome size of *T.*
108 *mercedesae* is the largest among those of mites whose genomes have been sequenced (*V. destructor*,
109 *Metaseiulus occidentalis*, *Tetranychus urticae*, *Sarcoptes scabiei*, and *Dermatophagoides farinae*) [6,
110 10-13] but smaller than those of ticks (for example, *Ixodes scapularis* [14]). As expected from the
111 largest genome size among the sequenced mites, gene density is low in the *T. mercedesae* genome
112 (with larger intergenic regions); reminiscent of the large velvet spider (*Stegodyphus mimosarum*) and
113 the black-legged tick (*I. scapularis*) genomes (Supplementary Fig. 3). Although the exon size range
114 was comparable in all tested genomes (small honey bee mite, predatory mite, black-legged tick,
115 velvet spider, spider mite, fruit fly, and honey bee) (Supplementary Fig. 4A), the average size of
116 introns in *T. mercedesae* is larger than that in two other mites and insects that were analyzed
117 (Supplementary Fig. 4B). We also successfully annotated genes encoding rRNA, tRNA, snRNA, and
118 miRNA in the *T. mercedesae* genome (Supplementary Table 6), obtained RNA-seq data from *T.*
119 *mercedesae* adult males and females as well as nymphs, and assembled the reads to aid
120 protein-coding gene annotation and to compare their gene expression profiles.

121 **Comparative genomics**

122 The protein-coding genes of *T. mercedesae* were compared with those of six other arthropods
123 (mentioned above) and a nematode. Phylogenetic trees constructed using 926 highly conserved 1:1
124 orthologs implementing both maximum likelihood and Bayesian methods demonstrated that the
125 *Tropilaelaps* mite and the predatory mite cluster together; however, the spider mite forms an
126 outgroup to two other mites, the black-legged tick, and the velvet spider (Fig. 1A). This is consistent
127 with previous reports that the subclass Acari is diphyletic, with the superorders Acariformes (spider
128 mite) and Parasitiformes (*Tropilaelaps* mite and predatory mite) being distantly related [15, 16].
129 Since above three mite species have similar body structure and morphology, this could be an
130 example of convergent evolution [17]. Based on this phylogenetic topology, we estimated that
131 parasitiform mites and ticks separated from other arachnids approximately 302 Mya as recently
132 reported [16] (Supplementary Fig. 5). The molecular species phylogenetic tree also indicates the
133 variable evolutionary rates in gene sequence; with the branch of *T. mercedesae* and *M. occidentalis*
134 exhibiting the fastest rate among arthropods we tested (Fig. 1A).

135 OrthoMCL classified the predicted proteins of *T. mercedesae* together with proteins from six
136 other arthropods into a total of 15,506 gene families. As expected from the phylogenetic tree, the
137 *Tropilaelaps* mite shares the most gene families (1,215) with the predatory mite (Fig. 1B). Among
138 these gene families, GO terms related with 'Structural constituent of cuticle', 'Regulation of DNA
139 methylation', and 'Xenobiotic metabolic process' are enriched (Supplementary Table 7). We found
140 119 gene families consisting of 332 species-specific genes, and 5,846 unclustered genes are present

141 in *T. mercedesae* but not in the other arthropods analyzed (Fig. 1A and B). Among these young
142 lineage-specific genes, three GO terms, 'Structural constituent of cuticle', 'Nucleosome', and 'DNA
143 bending complex' are highly enriched (FDR < 1.50 E⁻⁰⁴) (Supplementary Table 8). *T. mercedesae*
144 contains 117 members of the cuticle protein family [18], in which 53 are novel among the seven
145 arthropods analyzed, suggesting that the mite's exoskeleton has rapidly evolved. Two other enriched
146 GO terms could be involved in the epigenetic control of gene expression. Among 226 gene families
147 that are shared between *T. mercedesae*, *M. occidentalis*, and *I. scapularis*, GO terms related with
148 'Transporter activity' are highly enriched. We found that 135 gene families specifically shared
149 between *T. mercedesae* and *I. scapularis* were enriched with GO terms related to 'Renal tubule
150 development', perhaps to maintain a constant water level following the intake of a large volume of
151 hemolymph or blood, respectively [19, 20] (Supplementary Table 9).

152 We used CAFE to infer gene family expansion and contraction in *T. mercedesae* together with
153 six other arthropod species. We found that *T. mercedesae* has undergone the fewest gene family
154 expansion/contraction events since divergence from the common ancestor of arthropods
155 (Supplementary Fig. 6). This feature may fit to the specific life history of a mite parasitizing only the
156 honey bee and living inside a colony with an enclosed, stable environment. However, there are some
157 significantly expanded gene families (*P*-value < 0.001) associated with zinc ion binding and peptide
158 cross-linking. Meanwhile, one of the HSP70 gene families (Heat shock 70 kDa protein cognate 4)
159 has significantly contracted in *T. mercedesae* (Supplementary Table 10), perhaps because the mite
160 spends most of its time in the honey bee brood cell where the temperature is constantly around 35°C
161 [21]. We analyzed 91 genes with $d_N/d_S > 1.0$ in *T. mercedesae* using the one ratio model (null model)
162 to test the significance, and found that four genes have evolved rapidly either due to relaxation or
163 positive selection (Supplementary Table 11). Among them, Tm_07523 encodes an
164 endo-β-N-acetylglucosaminidase-like protein, a chitinase, which could be involved in processing
165 chitin specifically present in *T. mercedesae*.

166 **Sensory systems**

167 *T. mercedesae* has a very specific life history and habitat as a honey bee ectoparasitic mite. The mite
168 depends only on the honey bee as the host and spends most of its life in the capped brood cell. Thus,
169 they are likely to depend on the chemosensory rather than the visual system to seek out the fifth
170 instar honey bee larva and the mating pair. Therefore, we annotated and analyzed genes associated
171 with phototransduction and chemosensory systems in *T. mercedesae*.

172 We found that the homologs of *D. melanogaster* opsins, arrestin, TRPL, and INAD are absent in
173 *T. mercedesae* (Supplementary Fig. 7). Since they are the major components for fruit fly
174 photoreception, *T. mercedesae* appears to be blind, and this is consistent with the lack of eye
175 structures. Nevertheless, the adult females immediately move out from a brood cell when the cap is
176 removed and exposed to light, suggesting that they may be able to respond to light. *T. mercedesae*
177 has two *peropsin* genes, as do predatory mites [16] (Supplementary Fig. 8). Peropsin is a retinal
178 photoisomerase that converts all-*trans*-retinal to 11-*cis*-retinal and may couple with a G-protein
179 through the conserved 'NPXXY' motif at the seventh transmembrane domain [22]. The existence of
180 this gene in the jumping spider, black-legged tick, and humans suggests that peropsin may have been
181 lost specifically in insects. However, its function in vision or other pathways remains to be
182 determined. Only one of two *peropsin* genes (Tm_08036) appears to be expressed in the *T.*

183 *mercedesae* transcriptome, and it was highly expressed in the female compared to the male
184 (Supplementary Fig. 9). Female may use this peropsin to move out from the brood cell for
185 reproduction. The other components in phototransduction are present in *T. mercedesae*, suggesting
186 that they could be involved in other signaling pathways. In contrast to *T. mercedesae*, *M.*
187 *occidentalis* was reported to contain more molecular components for light perception such as
188 arrestins and INAD and exhibit genuine light-induced behaviors in the absence of eyes [16].
189 Meanwhile, *I. scapularis* contains seven opsins, including orthologs of the insect long-wavelength
190 sensitive visual opsins [23], demonstrating that the tick uses more visual cues for location of mates,
191 hosts and oviposition sites than the mites above.

192 Insect gustatory receptors (GRs) are multifunctional proteins for the perception of taste, airborne
193 molecules, and heat [24]; however, their functions in other arthropods have not been addressed. We
194 found only five GRs in *T. mercedesae* (TmGRs) without orthology to any *D. melanogaster* GRs (Fig.
195 2). *I. scapularis* has expanded the specific group of GRs [23], and five TmGRs cluster with the tick's
196 GRs, suggesting that these are expansions specific to Acari. Because they share a common ancestor
197 with the *D. melanogaster* sugar receptor, they could be involved in taste perception (Fig. 2). Among
198 the five TmGRs, one gene (Tm_15249) is likely to be a pseudogene due to internal stop codons in
199 the open reading frame. Expression of only two TmGR genes (Tm_03548 and Tm_09509) was
200 supported by RNA-seq data. Tm_09509 mRNA is highly expressed in adult females and Tm_03548
201 mRNA is only detected in males at low levels (Supplementary Fig. 10), suggesting that they may
202 respond to different ligands.

203 Ionotropic receptors (IRs) belong to a large family of ligand-gated ion channels, which also
204 include ionotropic glutamate receptors (iGluRs) with the major roles in synaptic transmission. IRs
205 appear to represent protostome-specific ancient olfactory and gustatory receptors [25]. We annotated
206 eight IR and 34 iGluR genes in the *T. mercedesae* genome. In the eight annotated *T. mercedesae* IR
207 (TmIR) genes, Tm_15231 and Tm_15229 are orthologs of DmIR25a and DmIR93a, respectively
208 (Supplementary Fig. 11), which are expressed in the olfactory sensory neurons of *D. melanogaster*
209 antennae [26]. Furthermore, DmIR25a has been recently shown to be involved in fruit fly
210 temperature sensation [27, 28]. The results of qRT-PCR revealed that these two genes are highly
211 expressed in the first legs of *T. mercedesae* (Supplementary Fig. 12), which function as the major
212 sensory organs similar to insect antennae [29]. Thus, these two TmIRs may represent the ancient
213 receptors present in the common ancestor of arthropods. It appears that six other TmIRs have arisen
214 specifically in a mite lineage (Supplementary Fig. 11).

215 Interestingly, there are no OR (olfactory receptor), OBP (odorant binding protein), and CSP
216 (chemosensory protein) genes in the *T. mercedesae* genome (Table 2). Since OR and OBP genes are
217 also absent in *M. occidentalis*, the black-legged tick, the centipede (*Strigamia maritima*), and the
218 water flea (*Daphnia pulex*), these appear to have evolved specifically in insect genomes as
219 previously suggested [30]. Nevertheless, CSP genes must be ancient and may have been specifically
220 lost in the two mite species. Despite of the potential importance of chemical communication for the
221 life cycle [4], *T. mercedesae* has only four functional GRs and eight IRs, but no OR, OBP, or CSP
222 genes. The presence of few orthologs between *T. mercedesae* and *D. melanogaster* suggests that the
223 last common ancestor of arthropods had very few GRs and IRs. These chemoreceptors appear to
224 have expanded in arthropod species in a lineage-specific manner [31]. In fact, Parasitiformes

225 exposed to more variable environments, *i.e.*, *M. occidentalis* and *I. scapularis*, have more GR and IR
226 genes than the more strictly host-dependent *T. mercedesae* (Table 2). Simplified behavioral patterns
227 under a dark and stable environment inside a honey bee colony and capped brood cell may have
228 reduced the number of tools in the sensory system in *T. mercedesae*.

229 **Detoxification system**

230 Three major groups of enzymes have important roles for metabolizing toxic xenobiotics in insects
231 and the acquisition of insecticide resistance; cytochrome P450s (P450s), glutathione-S-transferases
232 (GSTs), and carboxylesterases (CCEs) [32]. P450s and CCEs are also involved in the synthesis and
233 degradation of ecdysteroids, juvenile hormones, pheromones, and neurotransmitters [33, 34].
234 After the actions of P450s and CCEs followed by GSTs, the xenobiotics-derived polar compounds or
235 conjugates can be transported out of the cell by ATP-binding cassette transporters (ABC transporters)
236 [35]. In some cases, ABC transporters and others directly and efficiently transport xenobiotics out of
237 the cell without enzymatic modifications to prevent the exertion of toxicity [35]. Since various
238 natural and synthetic chemical compounds have been used to control honey bee mites, it is of
239 considerable interest to understand how *T. mercedesae* may detoxify such miticides and develop
240 resistance.

241 We manually annotated 56 *T. mercedesae* P450 (TmP450) genes in which 18 appeared to be
242 pseudogenes. In fact, the expression of none of these genes was supported by RNA-seq data. Thus, *T.*
243 *mercedesae* has only 38 apparently functional P450 genes similar to the human louse, *Pediculus*
244 *humanus* [36], and the expression of 36 genes were confirmed by RNA-seq data (Supplementary
245 Table 12). Similar to insect P450s, they are phylogenetically clustered into CYP2, CYP3, CYP4, and
246 mitochondrial clans (Fig. 3). The classification was based on *D. melanogaster* P450s, but only three
247 TmP450 genes (Tm11277, Tm11316, and Tm10252) have *D. melanogaster* P450 (DmP450)
248 orthologs classified as CYP2 and mitochondrial clans (Fig. 3 and Table 3). Thus, only a few P450
249 genes were present in the last common ancestor of arthropods and might be associated with the
250 synthesis and degradation of hormones. In the two large CYP3 and CYP4 clans, DmP450s and the
251 mite P450s are phylogenetically separated, suggesting that they have independently expanded after
252 the split of the ancestors of mites and insects (Fig. 3). All of the TmP450 genes have orthologs in the
253 *M. occidentalis* genome as recently reported [37], but *M. occidentalis* has 12 and 13 more genes than
254 *T. mercedesae* in the CYP2 and CYP3 clans, respectively, by our analysis (Table 3). *T. mercedesae*
255 appears to have lost the CYP3 clan members from the common ancestor of the Parasitiformes (Fig.
256 3) as suggested by CAFE analysis (Supplementary Table 13). Some of the TmP450 genes are
257 differentially expressed between nymph, adult male, and adult female (Supplementary Fig. 13 and
258 Supplementary Table 14), suggesting that they would be involved in the synthesis and degradation of
259 hormones to control molting and sex-specific phenotypes of *T. mercedesae*.

260 *T. mercedesae* has 15 GST genes (TmGST) in which eight appear to be pseudogenes without
261 evidences of the mRNA expression in the transcriptomes. This leads to only seven functional
262 TmGST genes with mRNA expression confirmed by RNA-seq data (Supplementary Table 15).
263 According to the reference data sets (*D. melanogaster* and *T. urticae* GSTs), the phylogenetic
264 analysis of TmGSTs revealed the presence of four subfamilies (delta, mu, omega, and kappa), and an
265 unclassified TmGST gene (Supplementary Fig. 14). Members in the mu, delta, epsilon, omega, theta,
266 and zeta GST subclasses have been reported to function in a wide range of detoxification [38].

267 Epsilon, sigma, theta, and zeta subfamilies are absent in both *T. mercedesae* and *M. occidentalis* by
268 our analysis in contrast to the recent report [37]; however, *I. scapularis* contains epsilon and zeta
269 subfamilies and *T. urticae* has the theta subfamily (Supplementary Table 16). This suggests that these
270 three subfamilies have been lost from the *T. mercedesae* and *M. occidentalis* genomes. The full
271 length orthologs of the five TmGST pseudogenes (Tm_05455, Tm_09167, Tm_15202, Tm_15203,
272 and Tm_15206) are present in *M. occidentalis* (Supplementary Fig. 14), suggesting that the delta and
273 mu GST subfamilies have undergone constriction in *T. mercedesae*.

274 Insect CCEs can be divided into 14 subfamilies (A to N) with three major groups based on the
275 functions of dietary detoxification (A-C), hormone and pheromone degradation (D-H), and
276 neurotransmitter degradation (I-N) [39]. We manually annotated 50 *T. mercedesae* CCE genes, in
277 which eight appeared to be pseudogenes without mRNA expression (Supplementary Table 17). The
278 number of functional CCE genes in *T. mercedesae* is thus comparable to that in *M. occidentalis* [37]
279 (Supplementary Table 18). Intriguingly, there are no mite CCEs in the subfamilies AF, H, I, K, and
280 N; however, a massive mite specific expansion is found in the subfamilies J and M by our analysis
281 (Supplementary Fig. 15 and Supplementary Table 18). Only three TmCCE genes (Tm_00126,
282 Tm_05721, and Tm_08305) have *D. melanogaster* orthologs, suggesting that CCE genes have
283 independently duplicated in insects and mites. The expression of some TmCCE genes is biased
284 between the nymph, adult female, and adult male (Supplementary Table 19). Above results
285 demonstrate that *T. mercedesae* contains P450s, GSTs, and CCEs although the number and
286 composition of subfamilies are different from those of other arthropods. Some of these enzymes may
287 engage in detoxifying miticides and other xenobiotics in *T. mercedesae*.

288 We annotated 54 ABC transporter genes in the *T. mercedesae* genome, and the expression of 47
289 genes was confirmed by RNA-seq data (Supplementary Table 20). Similarly, *M. occidentalis*
290 contains 57 ABC transporters that are comparable to those present in *D. melanogaster* (56 genes)
291 (Supplementary Table 20). However, mite-specific expansion is found in the ABCC subfamily, and
292 instead fruit fly-specific expansion is observed in the ABCG subfamily (Supplementary Fig. 16). The
293 ABCC subfamily includes many vertebrate multidrug-resistance associated proteins (MRPs) that
294 extrude drugs with broad specificity [35]; thus, the expanded ABCC subfamily members in *T.*
295 *mercedesae* could be involved in conferring resistance against various miticides. In the fruit fly,
296 expansion has been observed of the ABCG subfamily, which contains the transporters for the uptake
297 of pigment precursors into the cells of the Malpighian tubules and developing compound eyes
298 (Supplementary Fig. 16). Because these mites do not have eyes, fewer numbers of the ABCG
299 transporters would be sufficient. The mites and fruit fly appear to have independently expanded
300 ABCA subfamily members (Supplementary Fig. 16). These results suggest that most of the ABCA
301 and ABCC transporters may carry out different functions in mites and fruit flies. Interestingly, two
302 transporters, Tm_07059 and Tm_14842, form an independent clade separated from eight previously
303 known ABC transporter subfamilies. In cases where the mite ABC transporter genes show biased
304 expression between female, male, and nymph, most of them are highly expressed in either male or
305 nymph compared to female (Supplementary Table 21).

306 **Sex determination genes in *T. mercedesae***

307 Arthropods are known to use various strategies for sex determination [40]. In contrast to *T.*
308 *mercedesae*, which is likely to use haplodiploidy, *M. occidentalis* employs parahaploidy, in which the

309 functional elimination of paternal chromosomes occurs during early embryogenesis resulting in male
310 development [16, 41]. To gain insight into the mechanism of sex determination of *T. mercedesae*, we
311 manually annotated the candidate genes for sex determination in the *T. mercedesae* genome.
312 Similarly to *M. occidentalis* [16], *T. mercedesae* does not contain upstream sex determination genes
313 (*Sex-lethal* and *transformer*) but has the homologs of downstream sex determination genes,
314 *transformer-2*, *dmrt* (doublesex and mab3 related transcription factor), and *intersex*. *T. mercedesae*
315 has the most *dmrt* genes of the arthropods that we tested (Supplementary Table 22) and has two extra
316 *dsx* genes compared to *M. occidentalis* (Supplementary Fig. 17). The Dmrt93B ortholog is present in
317 *T. mercedesae* (Tm_07872) but not in *M. occidentalis* (Supplementary Fig. 17), and all of the *dmrt*
318 genes are highly expressed in the male (Supplementary Fig. 18). These results suggest that *T.*
319 *mercedesae* and *M. occidentalis* may use a different set of genes for sex determination.

320 **Comparison of gene expression profiles between nymphs and adult males and females**

321 Comparison between adult male and female transcriptomes and proteomes revealed that
322 histone-lysine-N-methyltransferase gene family and N-acetyltransferase *gcn5* gene family were
323 highly expressed in the male compared to the female (Fig. 4, Supplementary file 1, and
324 Supplementary Table 23), suggesting that the male mite may mostly depend on histone modifications
325 for the epigenetic control of gene expression. This could be due to the ploidy compensation between
326 males with haploid genomes and females with diploid genomes. At the protein level, males displayed
327 overrepresentation of 26S proteasome subunits and a 17-beta-hydroxysteroid dehydrogenase (Fig. 4),
328 which accords with the importance of the ubiquitin-proteasome system in sperm maturation [42] and
329 a potential role for ecdysteroids in sexual maturation of *T. mercedesae* [43]. The female mite highly
330 expresses the vitellogenin gene family and cathepsin L-like proteases (Fig. 4 and Supplementary
331 Table 23). This is consistent with active oogenesis in female mites, since both vitellogenin protein
332 and Nanos mRNA would be deposited in the oocyte; while cathepsin L proteases may have a critical
333 role in yolk processing as in *C. elegans* [44]. The results of above transcriptome and proteome
334 analyses are not identical but a concordant set of 74 and 13 genes are up-regulated in the male and
335 females, respectively. Comparison between adult female and nymph transcriptomes demonstrated
336 that 46 out of the 125 cuticle protein gene families, 13 out of 24 chitin binding domain-containing
337 protein gene families, and nine out of 16 chitinase gene families are expressed at a higher level in
338 nymphs than in adult females (Supplementary Table 24), indicating that chitin metabolism as well as
339 exoskeleton formation by molting is stimulated in the nymph. The nymph also highly expresses 18
340 out of 29 protocadherin/fat gene families and 18 out of 44 epidermal growth factor-related receptor
341 gene families. These are likely to be involved in cell-cell adhesion and cell proliferation associated
342 with the increase of cell number in nymph. Consistent with above results, GO analysis of genes
343 highly expressed in nymphs compared to the adult females demonstrated that many GO terms related
344 to cuticle formation and appendage morphogenesis are enriched (Supplementary Table 25).

345 **Symbiotic bacteria and infecting virus**

346 Several bacteria have been shown to associate with mites and ticks [12, 45, 46]; however, bacteria
347 associated with honey bee mites have not yet been fully investigated [6]. We thus attempted to
348 identify any bacteria associated with *T. mercedesae* by filtering the bacteria-derived DNA contigs
349 during the mite genome assembly. In the male and female GC%-coverage plots, some contigs were
350 initially annotated as bacterial DNA in the major blue blob, and most of these were identified to

351 contain *Wolbachia* sequences by BLASTN searches (Fig. 5). By testing the mite genomic DNA
352 organization in two such contigs by PCR with two sets of primers (one primer located in the mite
353 gene, and the other in the *Wolbachia* gene), we found that parts of *Wolbachia* genes are integrated
354 into the mite genome, most likely by horizontal transfer (Supplementary Fig. 19A and B). This
355 phenomenon of nuclear *Wolbachia* transfers, or *nuwts*, has been observed widely in other arthropods
356 and in nematodes [47], although to the best of our knowledge, this is the first report for a chelicerate.
357 Meanwhile, we extracted all reads mapped to the red blob (bacterial origin) in the female plot (Fig.
358 5) and re-assembled them into 96 contigs. We annotated 751 protein-coding genes from the 81
359 contigs and found that 667 of these show high similarity to those of *Rickettsiella grylli* with an
360 average identity of 79%. The rest of the 84 protein-coding genes showed similarity to 20 other
361 bacteria species, such as *Diplorickettsia massiliensis* and *Legionella longbeachae*. This demonstrates
362 that a close relative of *R. grylli* associates with female but not male *T. mercedesae*. *Rickettsiella* is an
363 intracellular gamma-proteobacterium associated with a wide range of different arthropods without
364 major pathogenicity to the host [48]. *Wolbachia* might be replaced by a species related to *R. grylli* in
365 *T. mercedesae*. The potential effects on *T. mercedesae* as well as the potential for transmission to the
366 honey bee remain to be determined. Since we did not find any DNA sequences of actinomycete
367 species in our sequence reads, the two major ectoparasitic mites of honey bee (*V. destructor* and *T.*
368 *mercedesae*) do not appear to share the same bacteria [6]. Nevertheless, both mites do not contain
369 common arthropod gut bacteria, suggesting that they are not essential for the honey bee mites.

370 We also assembled DWV (deformed wing virus) RNA in the adult male and female, as well as
371 nymph, transcriptomes (Supplementary Table 26). This is consistent with previous reports [49-51];
372 however, our data expand the infected stages to include the adult males and nymphs. DWV sequence
373 reads represented one third of the whole RNA-seq data, and these very high levels of DWV RNA
374 were further confirmed by qRT-PCR (Supplementary Table 27). The proteomic analysis of females
375 and males recovered many peptides derived from the capsid (structural) proteins, but very few
376 peptides from the non-structural proteins of DWV, demonstrating that the majority of DWV
377 associated with the mites exists as mature virions (Supplementary Fig. 20). Similar observations
378 were also reported for *V. destructor* [52]. We assembled three full length DWV RNA genomes and
379 found that they are phylogenetically clustered with type A DWV [53] (Fig. 6). Thus, *T. mercedesae*
380 may spread the specific strain of DWV (type A in this study) to honey bees as suggested for *V.*
381 *destructor* [54]. Considering that *T. mercedesae* was unlikely to carry DWV when associated with
382 the original host, *A. dorsata*, DWV infection could impose a negative impact on the mite. It will be
383 crucial to understand the nature of interactions between honey bee, mite, and DWV to measure the
384 impact of *T. mercedesae* infestation on honey bee colonies. However, in contrast to *V. destructor*, we
385 did not detect baculoviruses in either the genome and transcriptome sequences [6].

387 Conclusions

388 *T. mercedesae* has a very specialized life history and habitat as an ectoparasitic mite strictly
389 depending on honey bees in a colony with closed and stable environment. Thus, comparison of the
390 genome and transcriptome sequences with those of a free-living mite and a tick has revealed the
391 specific features of the genome shaped by interaction with the honey bee and colony environment.
392 Our key findings are the followings;

- 393 1) Amino acid substitutions have been accelerated within the conserved core genes of *T. mercedesae*
394 and *M. occidentalis*
395 2) *T. mercedesae* has undergone the least gene family expansion and contraction between the seven
396 arthropods we tested
397 3) The numbers of HSP70 family genes and sensory system genes are reduced
398 4) *T. mercedesae* may have evolved a specialized cuticle and water homeostasis mechanisms, as well
399 as epigenetic control of gene expression for ploidy compensation between male and female
400 5) *T. mercedesae* contains all gene sets required to detoxify xenobiotics, enabling it to be miticide
401 resistant
402 6) *T. mercedesae* is closely associated with a symbiotic bacterium (*Rickettsiella grylli*-like) and
403 DWV, the most prevalent honey bee virus.

404
405 Manipulation of symbiotic *R. grylli*-like bacteria in the female mites may give the opportunity to
406 control *T. mercedesae* in the future. Our *T. mercedesae* datasets, alongside published *V. destructor*
407 genome and transcriptome sequences, not only provide insights into mite biology, but may also help
408 to develop measures to control the most serious pests of the honey bee.

409 410 **Methods**

411 **Mite sample collection**

412 Based on the morphological and ethological characteristics [55], adult males and females as well as
413 nymphs of *T. mercedesae* were identified and collected from a single honey bee colony for the flow
414 cytometric analysis and Illumina sequencing (genome and transcriptome). Meanwhile, the adult
415 females #2 sample (Supplementary Table 1) was collected from a different colony. Both colonies
416 were obtained from a beekeeper in Jiangsu Province, China. The mites collected for genome
417 sequencing and proteomic characterization were stored in acetone at 4°C until use. The mites used
418 for RNA-seq were sorted at -80°C before the transport with dry ice.

419 **Genome and transcriptome sequencing**

420 Before DNA extraction, the mite bodies were carefully washed twice with acetone to remove any
421 non-target organisms that might adhere on the mite surface. Subsequently, a single male and a single
422 female mite were air dried (15 min) and individually triturated in 180 µL of lysozyme buffer (1M
423 Tris-HCl, 0.5M EDTA, 1.2% Triton X-100, and 0.02% lysozyme) with a tissuelyser II (Qiagen,
424 Valencia, CA) using a 3 mm stainless steel bead at 25,000 motions/min for 30 sec. After incubating
425 the samples at 37 °C for 30 min, total DNA was extracted from each of the triturated samples with
426 DNeasy Blood and Tissue kit (Qiagen) by following the manufacturer's spin-column protocol for
427 animal tissue. To maximize the yield of DNA extraction, two successive elution steps, each with 50
428 µl elution buffer, were performed. The DNA concentrations were determined by spectrophotometry,
429 a sensitive and commonly used fluorescent dye assay (Qubit® dsdna BR assay, Life Technologies
430 Europe, Naerum, Denmark) according to the manufacturer's instructions. Illumina HiSeq 2500
431 sequencing was carried out in the Centre for Genomic Research at the University of Liverpool. Male,
432 female and nymph mites (each with 20~30) were shipped to BGI tech for total RNA extraction,
433 polyA⁺ RNA enrichment, cDNA library preparation, and Illumina Hiseq 2000/4000 sequencing

434 **Estimation of genome size and ploidy of *T. mercedesae***

435 Nuclear DNA contents of *T. mercedesae* males and females were estimated by a method of
436 propidium iodide staining followed by flow cytometry [14]. Nuclei were isolated from ten *T.*
437 *mercedesae* adult males and females, the heads of ten *D. melanogaster* females (1C = 175Mb) [56]
438 and the brain of a honey bee worker (1C = 262 Mb) [57]. Stained nuclei from adult male and female
439 mites were independently analyzed with two reference standards using a BD FACS flow cytometer
440 (BD Biosciences, San Jose, CA). Nuclear genome size was then calculated according to the
441 following formula: Sample nuclear DNA content = (Mean peak of sample/Mean peak of reference
442 standard) × nuclear DNA content of reference standard. We estimated the genome size by analyzing
443 the frequency of *k*-mers counted by Jellyfish [58] with the following formula [59]: Estimated
444 genome size (bp) = total number of *k*-mer/the maximal frequency. The ploidy is the ratio of nuclear
445 DNA content to genome size.

446 **De novo assembly of genomic DNA**

447 DNA sequences derived from non-targets such as bacteria and mitochondria were filtered out based
448 on the preliminarily male and female genomes assembled by Velvet [60] using a GC-coverage
449 (proportion of GC bases and node coverage) plot-based method (Fig. 5). The sequence reads mapped
450 to the *A. mellifera* genome [57] were also removed. The cleaned reads of from the male were
451 re-assembled and optimized up to scaffold level using the VelvetOptimiser.

452 **Genome annotation**

453 To find and classify repeated sequences in the assembled genome, a *de novo* repeat library was first
454 built using Repeatmodeler (A. F. A. Smit and P. Green, unpublished) followed by Repeatmasker (A.
455 F. A. Smit and P. Green, unpublished). Then, a homology-based prediction of repeated sequences in
456 the genome was achieved using Repeatmasker and a known repeat library issued on January 13,
457 2014. For non-interspersed repeated sequences, we ran Repeatmasker with the ‘-noint’ option, which
458 is specific for simple repeats, micro satellites, and low-complexity repeats. Tandem repeats in the
459 genome were scanned with the TRF program (v4.04) [61].

460 RNA-seq reads obtained from all samples were aligned to the masked genomic scaffolds to
461 determine the exon-intron junctions using Tophat (v2.011) [62]. Cufflinks (v0.8.2) [63] used the
462 spliced alignments to reconstruct 44,614 transcripts from which 12,298 transcripts with intact coding
463 sequences were selected to train three *de novo* gene prediction programs. Augustus (v3.0.3) [64],
464 SNAP (v2013-11-29) [65], and Genemark (v2.3e) [66] predicted 32,561, 67,258, and 79,928 gene
465 models, respectively (Supplementary Table 2). We used BLASTN to map the assembled transcript
466 sequences onto the mite genome, and aligned the invertebrate RefSeq protein sequences
467 (downloaded on May 17, 2014 from NCBI) with the genomic scaffolds using BLASTX. Maker
468 integrated data from *de novo* gene prediction, and protein/transcript alignment was used to produce
469 integrated gene sets with high quality [67]. Genes identified by *de novo* prediction, which did not
470 overlap with any genes in the integrated gene sets, were also added to the gene set if they showed
471 significant hits (BLASTP E-value < 1e-5) to SwissProt proteins or could be annotated by
472 Interproscan (v4.8) [68] with superfamily database.

473 **ncRNA annotation**

474 In this analysis, we annotated four types of ncRNA: transfer RNA (tRNA), ribosomal RNA (rRNA),
475 microRNA, and small nuclear RNA (snRNA). Genes encoding tRNA were predicted by tRNAscan-SE
476 (v1.3.1) [69] with eukaryote parameters, and rRNA genes were identified by aligning the rRNA

477 template sequences from invertebrates (database: SILVA 119) to the *T. mercedesae* genomic DNA
478 using BLASTN with an E-value cutoff of 1e-5. Genes encoding miRNA and snRNA were inferred
479 by the Infernal software (v1.1.1) [70] using release 12 of the Rfam database.

480 **Protein functional annotation**

481 We performed the initial and principal domain annotation with the Pfam database (release 27) using
482 the HMMER hmmscan script with default settings. Additional domains were assigned using
483 InterProScan with superfamily, Gene3d, Tigrfams, Smart, Prosite, and Prints domain models. The
484 domain/motif based GO term was also obtained through InterProScan searches.

485 We used Blast2GO pipeline (v2.5) [71] to further annotate proteins by Gene Ontology (GO)
486 terms. In the first step, we searched the nr database with BLASTP using a total of 17,508 protein
487 sequences as queries. The E-value cutoff was set at 1e-6 and the best 20 hits were collected for
488 annotation. Based on the BLAST results, Blast2GO pipeline then predicted the functions of proteins
489 to assign GO terms, and merged the InterProScan deduced domain/motif based GO terms into these
490 BLAST based annotations.

491 The metabolic pathway was constructed based on the KAAS (KEGG Automatic Annotation
492 Server) online server [72] using the recommended eukaryote sets, all other available insects, and *I.*
493 *scapularis*. The pathways in which each gene product might be involved were derived from the best
494 KO hit with BBH (bi-directional best hit) method.

495 **GO enrichment**

496 We performed the GO enrichment analyses of gene sets with Fisher's exact test embedded in the
497 Blast2GO desktop version (v2.8). If not specifically stated, the *P*-values were corrected according to
498 the critical FDR. The enrichments were tested by comparing the GO terms with the pooled set of GO
499 terms of all *T. mercedesae* proteins.

500 **Construction of phylogenetic trees**

501 We first aligned orthologous protein sequences with Mafft (v7.012b) [73] or Kalign (v2.0) [74], and
502 then used Gblocks (v0.91b) [75] to automatically eliminate the divergent regions or gaps prior to
503 phylogenetic analysis. However, we manually trimmed the aligned sequences for big gene sets. The
504 best substitution models of amino acid substitution were determined for the alignments by Prottest
505 (v3.4) with parameters set to “-all-matrices, -all-distributions, -AIC” [76]. Then, phylogenetic trees
506 were constructed using maximum likelihood methods (Phyml, v3.1) [77] or Bayesian methods
507 (MrBayes, v3.2.3) [78]. In addition, a neighbor-joining method was also used for building the
508 distance-based trees using MEGA (v6.06) [79].

509 **Evolutionary analyses**

510 Protein data sets of the following arthropod genomes were used as references: *D. melanogaster* (fruit
511 fly; GOS release: 6.03) [80], *A. mellifera* (honey bee; GOS release: 3.2) [57], *T. urticae* (spider mite;
512 GOS release: 20140320) [10], *Stegodyphus mimosarum* (velvet spider; GOS release: 1.0) [81], *I.*
513 *scapularis* (black-legged tick; GOS release: 1.4) [23], *M. occidentalis* (predatory mite; GOS release:
514 1.0) [16]. *Caenorhabditis elegans* (nematode; GOS release: WS239) [82] was used as the outgroup.
515 Domain, GO, and KEGG annotation of proteins in the reference species (if required) was conducted
516 using the same methods as those used for *T. mercedesae*.

517 Since the rapid evolution of acariform mites may challenge phylogenetic analyses due to
518 long-branch attraction [83], we used a very strict E-value (1e-50) when performing a reciprocal

BLASTP to gate out the most variant orthologous genes across all genomes tested. The reciprocal BLAST search resulted in identification of a total of 926 highly conserved one-to-one orthologs in all eight genomes. Each of these orthologous groups was aligned using Mafft in “-auto” option. These alignments were trimmed by Gblocks and concatenated into the unique protein superalignments before conducting the phylogenetic analysis with both Phyml and MrBayes.

Based on the topology defined by phylogenetic analysis above, we estimated the divergence time of each species using the Bayesian MCMC method in the PAML package (v4.7) [84] together with information from several fossil records (Mya): tick-spider: 311–503 [81] (oldest spider from coal, UK), *T. urticae*-tick-spider: 395–503 [81] (oldest Acari), *A. mellifera*-*D. melanogaster*: 238–307 (<http://www.fossil-record.net/>) and nematode-arthropods: 521–581 (<http://www.fossil-record.net/>).

Orthologous gene families between *T. mercedesae* and six reference arthropods were defined using OrthoMCL (v1.4) [85]. We used CAFE (v3.1) [86] to infer the gene family expansion and contraction in *T. mercedesae* against all reference arthropods or against Parasitiformes (*I. scapularis* and *M. occidentalis*). We also calculated ω (d_N/d_S) ratios for 1,865 one-to-one orthologs defined by OrthoMCL using Codeml in the PAML package with the free-ratio model. Branches with $\omega > 1$ are considered under positive selection. The null model used for branch test was the one-ratio model, where ω was the same for all branches. Measurement of d_S was assessed by substitution saturation, and only d_S values < 3.0 were retained for the analysis of positive selection. Genes with high ω ratio (>10) were also discarded.

Analysis of RNA-seq data

We first aligned the clean RNA-seq reads to the assembled *T. mercedesae* genome using Tophat. Then, Htseq-count in the Htseq Python package (v0.6.1) [87] was used to obtain raw read counts, with the default union-counting mode and option ‘-a’ to specify the minimum score for the alignment quality. The raw read count for each sample was then subject to further differential expression analysis using the EdgeR (v3.0) Bioconductor package [88]. We excluded mRNAs without at least one count per million in the replicates (low overall sum of counts) from the analyses as previously suggested [89]. We then normalized the library sizes of all samples according to the trimmed mean of M-values method, and dispersion was estimated from the replicates. Pairwise comparisons of differential gene expression between the RNA-seq samples were performed using the function of Exact test [90] with a FDR P -value cut-off 0.01.

qRT-PCR

We carried out qRT-PCR reactions, each in triplicate, using an Applied Biosystems 7500 Fast Real-Time PCR System and 2X KAPA SYBR FAST qPCR Master Mix (KAPA Biosystems Woburn, MA). To perform the absolute quantification of DWV RNA, we first prepared standard curves for DNA corresponding to DWV target RNA. The target DNA was prepared by PCR followed by the gel extraction. The DNA concentration was measured using Nanodrop 2000 spectrophotometer (Thermo Scientific, USA) to calculate the original copy number by a formula; Copy number = DNA concentration (ng/ μ l) \times 6.02 \times 10²³ (copies/mol) / length (bp) \times 6.6 \times 10¹¹ (ng/mol), in which 6.6 \times 10¹¹ ng/mol is the average molecular mass of one base pair, and 6.022 \times 10²³ copies/mol is the Avogadro’s number. Linear standard curves were then generated using target DNA of 10⁵–10⁹ copy number per reaction followed by plotting the Ct values against log values of the copy number. After

reverse transcription, the copy number of target RNA in a sample was estimated using the standard curve above. To carry out the relative quantification, we compared the relative expression levels of the target mRNA to *Ef-1α* mRNA as the internal reference using the $2^{-\Delta\Delta Ct}$ method. All primers used for qRT-PCR are listed in Supplementary Table 28.

Proteomic analysis

Pools of male or female ites were lysed by sonication in 0.1 % (w/v) Rapigest (Waters MS technologies) in 50 mM ammonium bicarbonate. Samples were heated at 80 °C for 10 min, reduced with 3 mM DTT at 60 °C for 10 min, cooled, then alkylated with 9 mM iodoacetamide (Sigma) for 30 min (room temperature) protected from light; all steps were performed with intermittent vortex-mixing. Proteomic-grade trypsin (Sigma) was added at a protein:trypsin ratio of 50:1 and incubated at 37 °C overnight. Rapigest was removed by adding TFA to a final concentration of 1 % (v/v) and incubating at 37 °C for 2 hours. Peptide samples were centrifuged at 12,000 x g for 60 min (4 °C) to remove precipitated Rapigest. The peptide supernatant was desalted using C₁₈ reverse-phase stage tips (Thermo Scientific) according to the manufacturer's instructions. Samples were desalted and reduced to dryness as above and re-suspended in 3 % (v/v) acetonitrile, 0.1 % (v/v) TFA for analysis by MS.

Peptides were analysed by on-line nanoflow LC using the nanoACQUITY-nLC system (Waters MS technologies) coupled with Q-Exactive mass spectrometer (Thermo Scientific). Samples were loaded on a 50cm Easy-Spray column with an internal diameter of 75 μm, packed with 2 μm C₁₈ particles, fused to a silica nano-electrospray emitter (Thermo Scientific). The column was operated at a constant temperature of 35 °C. Chromatography was performed with a buffer system consisting of 0.1 % formic acid (buffer A) and 80 % acetonitrile in 0.1 % formic acid (buffer B). The peptides were separated by a linear gradient of 3.8 – 50 % buffer B over 90 minutes at a flow rate of 300 nl/min. The Q-Exactive was operated in data-dependent mode with survey scans acquired at a resolution of 70,000. Up to the top 10 most abundant isotope patterns with charge states +2, +3 and/or +4 from the survey scan were selected with an isolation window of 2.0Th and fragmented by higher energy collisional dissociation with normalized collision energies of 30. The maximum ion injection times for the survey scan and the MS/MS scans were 250 and 50 ms, respectively, and the ion target value was set to 1E6 for survey scans and 1E5 for the MS/MS scans. Repetitive sequencing of peptides was minimized through dynamic exclusion of the sequenced peptides for 20s.

Thermo RAW files were imported into Progenesis LC-MS (version 4.1, Nonlinear Dynamics). Runs were time aligned using default settings and using an auto selected run as reference. Peaks were picked by the software using default settings and filtered to include only peaks with a charge state between +2 and +7. Spectral data were converted into .mgf files with Progenesis LC-MS and exported for peptide identification using the Mascot (version 2.3.02, Matrix Science) search engine. Tandem MS data were searched against translated ORFs from *T. mercedesae*, *Apis mellifera* (OGSv3.2) [91] and Deformed Wing Virus (Uniprot 08 2016) (total; 30,666 sequences; 12,194,618 residues). The search parameters were as follows: precursor mass tolerance was set to 10 ppm and fragment mass tolerance was set as 0.01Da. Two missed tryptic cleavages were permitted. Carbamidomethylation (cysteine) was set as a fixed modification and oxidation (methionine) set as variable modification. Mascot search results were further validated using the machine learning algorithm Percolator embedded within Mascot. The Mascot decoy database function was utilised and

603 the false discovery rate was < 1%, while individual percolator ion scores >13 indicated identity or
604 extensive homology ($P < 0.05$). Mascot search results were imported into Progenesis LC-MS as
605 XML files. Peptide intensities were normalised against the reference run by Progenesis LC-MS and
606 these intensities are used to highlight relative differences in protein expression between samples. The
607 mass spectrometry proteomics data have been deposited to the ProteomeXchange Consortium via the
608 PRIDE [92] partner repository with the dataset identifier PXD004997.

609 610 **Data availability**

611 All sequence data we obtained and analyzed are deposited under the project accession number
612 PRJNA343868 in NCBI.

613 614 **Additional files**

615
616 Supplementary file 1

617
618 Supplementary Tables

619
620 Supplementary Figures

621 622 **Abbreviations**

623 CCE: Carboxylesterase; CSP: Chemosensory protein; CYP: Cytochrome P450; ABC transporter:
624 ATP-binding cassette transporter; GR: Gustatory receptor; GST: Glutathione-S-transferase; IR:
625 Ionotropic receptor; OBP: Odorant binding protein; OR: Olfactory receptor; P450: Cytochrome
626 P450; DWV: Deformed wing virus; MS: Mass spectrometry.

627 628 **Competing interests**

629 We declare no competing interests.

630 631 **Authors' contributions**

632 XD conducted all experiments except the proteomic analyses which were carried out by SDA and
633 DX. TK, ACD, and BLM planned and supervised the research. XD and TK wrote the manuscript,
634 which was revised by ACD and BLM.

635 636 **Acknowledgements**

637 This work was supported in part by 2012 Suzhou Science and Technology Development Planning
638 Programme (Grant#: SYN201213) and Jinji Lake Double Hundred Talents Programme to TK. We
639 thank the Centre for Genomic Research at the University of Liverpool for *Tropilaelaps* mite genome
640 sequencing and Frances Blow for helping to construct the DNA libraries. We are grateful to local bee
641 keepers in Jiangsu province for providing honey bee colonies.

642 643 **References**

- 644 1. Vanengelsdorp D, Meixner MD: A historical review of managed honey bee populations in
645 Europe and the United States and the factors that may affect them. *J Invertebr Pathol* 2010,
646 103 Suppl 1:S80-95.
- 647 2. Evans JD, Schwarz RS: Bees brought to their knees: microbes affecting honey bee health.

645 *Trends in Microbiology* 2011, 19:614-620.

646 3. Rosenkranz P, Aumeier P, Ziegelmann B: Biology and control of Varroa destructor. *Journal*
647 *of invertebrate pathology* 2010, 103 Suppl 1:S96-119.

648 4. Anderson DL, Roberts JMK: Standard methods for Tropilaelaps mites research. *Journal of*
649 *Apicultural Research* 2013, 52.

650 5. Oldroyd BP: Coevolution while you wait: Varroa jacobsoni, a new parasite of western
651 honeybees. *Trends Ecol Evol* 1999, 14:312-315.

652 6. Cornman SR, Schatz MC, Johnston SJ, Chen YP, Pettis J, Hunt G, Bourgeois L, Elsik C,
653 Anderson D, Grozinger CM, Evans JD: Genomic survey of the ectoparasitic mite Varroa
654 destructor, a major pest of the honey bee Apis mellifera. *BMC Genomics* 2010, 11:602.

655 7. Parra G, Bradnam K, Korf I: CEGMA: a pipeline to accurately annotate core genes in
656 eukaryotic genomes. *Bioinformatics* 2007, 23:1061-1067.

657 8. Simão FA, Waterhouse RM, Ioannidis P, Kriventseva EV, Zdobnov EM: BUSCO: assessing
658 genome assembly and annotation completeness with single-copy orthologs. *Bioinformatics*
659 2015, 31:3210-3212.

660 9. Xu X, Pan S, Cheng S, Zhang B, Mu D, Ni P, Zhang G, Yang S, Li R, Wang J, et al: Genome
661 sequence and analysis of the tuber crop potato. *Nature* 2011, 475:189-195.

662 10. Grbic M, Van Leeuwen T, Clark R, Rombauts S, Rouze P, Grbic V, Osborne E, Dermauw W,
663 Phuong C, Ortego F, et al: The genome of Tetranychus urticae reveals herbivorous pest
664 adaptations. *Nature* 2011, 479:487-492.

665 11. Jeyaprakash A, Hoy MA: The nuclear genome of the phytoseiid Metaseiulus occidentalis
666 (Acari: Phytoseiidae) is among the smallest known in arthropods. *Exp Appl Acarol* 2009,
667 47:263-273.

668 12. Chan TF, Ji KM, Yim AK, Liu XY, Zhou JW, Li RQ, Yang KY, Li J, Li M, Law PT, et al: The
669 draft genome, transcriptome, and microbiome of Dermatophagoides farinae reveal a broad
670 spectrum of dust mite allergens. *J Allergy Clin Immunol* 2015, 135:539-548.

671 13. Rider SD, Morgan MS, Arlian LG: Draft genome of the scabies mite. *Parasit Vectors* 2015,
672 8:585.

673 14. Geraci NS, Spencer Johnston J, Paul Robinson J, Wikel SK, Hill CA: Variation in genome
674 size of argasid and ixodid ticks. *Insect Biochem Mol Biol* 2007, 37:399-408.

675 15. Gu XB, Liu GH, Song HQ, Liu TY, Yang GY, Zhu XQ: The complete mitochondrial genome
676 of the scab mite Psoroptes cuniculi (Arthropoda: Arachnida) provides insights into Acari
677 phylogeny. *Parasit Vectors* 2014, 7:340.

678 16. Hoy MA, Waterhouse RM, Wu K, Estep AS, Ioannidis P, Palmer WJ, Pomerantz AF, Simão
679 FA, Thomas J, Jiggins FM, et al: Genome Sequencing of the Phytoseiid Predatory Mite
680 Metaseiulus occidentalis Reveals Completely Atomized Hox Genes and Superdynamic Intron
681 Evolution. *Genome Biol Evol* 2016, 8:1762-1775.

682 17. Stern D: The genetic causes of convergent evolution. *Nature Reviews Genetics* 2013,
683 14:751-764.

684 18. Charles JP: The regulation of expression of insect cuticle protein genes. *Insect Biochem Mol*
685 *Biol* 2010, 40:205-213.

686 19. KAUFMAN W, AESCHLIMANN A, DIEHL P: REGULATION OF BODY VOLUME BY

- 687 SALIVATION IN A TICK CHALLENGED WITH FLUID LOADS. *American Journal of*
688 *Physiology* 1980, 238:R102-R112.
- 689 20. SAUER J, MCSWAIN J, BOWMAN A, ESSENBERG R: TICK SALIVARY-GLAND
690 PHYSIOLOGY. *Annual Review of Entomology* 1995, 40:245-267.
- 691 21. Tautz J, Maier S, Groh C, Rössler W, Brockmann A: Behavioral performance in adult honey
692 bees is influenced by the temperature experienced during their pupal development. *Proc Natl*
693 *Acad Sci U S A* 2003, 100:7343-7347.
- 694 22. Nagata T, Koyanagi M, Tsukamoto H, Terakita A: Identification and characterization of a
695 protostome homologue of peropsin from a jumping spider. *J Comp Physiol A Neuroethol*
696 *Sens Neural Behav Physiol* 2010, 196:51-59.
- 697 23. Gulia-Nuss M, Nuss AB, Meyer JM, Sonenshine DE, Roe RM, Waterhouse RM, Sattelle DB,
698 de la Fuente J, Ribeiro JM, Megy K, et al: Genomic insights into the Ixodes scapularis tick
699 vector of Lyme disease. *Nat Commun* 2016, 7:10507.
- 700 24. Joseph RM, Carlson JR: Drosophila Chemoreceptors: A Molecular Interface Between the
701 Chemical World and the Brain. *Trends Genet* 2015.
- 702 25. Croset V, Rytz R, Cummins SF, Budd A, Brawand D, Kaessmann H, Gibson TJ, Benton R:
703 Ancient protostome origin of chemosensory ionotropic glutamate receptors and the evolution
704 of insect taste and olfaction. *PLoS Genet* 2010, 6:e1001064.
- 705 26. Rytz R, Croset V, Benton R: Ionotropic receptors (IRs): chemosensory ionotropic glutamate
706 receptors in Drosophila and beyond. *Insect Biochem Mol Biol* 2013, 43:888-897.
- 707 27. Chen C, Buhl E, Xu M, Croset V, Rees JS, Lilley KS, Benton R, Hodge JJ, Stanewsky R:
708 Drosophila Ionotropic Receptor 25a mediates circadian clock resetting by temperature.
709 *Nature* 2015, 527:516-520.
- 710 28. Ni L, Klein M, Svec KV, Budelli G, Chang EC, Ferrer AJ, Benton R, Samuel AD, Garrity PA:
711 The Ionotropic Receptors IR21a and IR25a mediate cool sensing in Drosophila. *Elife* 2016, 5.
- 712 29. Cruz MDS, Robles MCV, Jespersen JB, Kilpinen O, Birkett M, Dewhirst S, Pickett J:
713 Scanning electron microscopy of foreleg tarsal sense organs of the poultry red mite,
714 *Dermanyssus gallinae* (DeGeer) (Acari : Dermanyssidae). *Micron* 2005, 36:415-421.
- 715 30. Robertson HM, Warr CG, Carlson JR: Molecular evolution of the insect chemoreceptor gene
716 superfamily in Drosophila melanogaster. *Proc Natl Acad Sci U S A* 2003, 100 Suppl
717 2:14537-14542.
- 718 31. Chipman AD, Ferrier DE, Brena C, Qu J, Hughes DS, Schröder R, Torres-Oliva M, Znassi N,
719 Jiang H, Almeida FC, et al: The first myriapod genome sequence reveals conservative
720 arthropod gene content and genome organisation in the centipede *Strigamia maritima*. *PLoS*
721 *Biol* 2014, 12:e1002005.
- 722 32. Li X, Schuler MA, Berenbaum MR: Molecular mechanisms of metabolic resistance to
723 synthetic and natural xenobiotics. *Annu Rev Entomol* 2007, 52:231-253.
- 724 33. Iga M, Kataoka H: Recent studies on insect hormone metabolic pathways mediated by
725 cytochrome P450 enzymes. *Biol Pharm Bull* 2012, 35:838-843.
- 726 34. Toutant JP: Insect acetylcholinesterase: catalytic properties, tissue distribution and molecular
727 forms. *Prog Neurobiol* 1989, 32:423-446.
- 728 35. Dermauw W, Van Leeuwen T: The ABC gene family in arthropods: comparative genomics

- 729 and role in insecticide transport and resistance. *Insect Biochem Mol Biol* 2014, 45:89-110.
- 730 36. Kirkness EF, Haas BJ, Sun W, Braig HR, Perotti MA, Clark JM, Lee SH, Robertson HM,
731 Kennedy RC, Elhaik E, et al: Genome sequences of the human body louse and its primary
732 endosymbiont provide insights into the permanent parasitic lifestyle. *Proc Natl Acad Sci U S*
733 *A* 2010, 107:12168-12173.
- 734 37. Wu K, Hoy MA: The Glutathione-S-Transferase, Cytochrome P450 and
735 Carboxyl/Cholinesterase Gene Superfamilies in Predatory Mite *Metaseiulus occidentalis*.
736 *PLoS One* 2016, 11:e0160009.
- 737 38. Enayati AA, Ranson H, Hemingway J: Insect glutathione transferases and insecticide
738 resistance. *Insect Mol Biol* 2005, 14:3-8.
- 739 39. Yu QY, Lu C, Li WL, Xiang ZH, Zhang Z: Annotation and expression of carboxylesterases in
740 the silkworm, *Bombyx mori*. *BMC Genomics* 2009, 10:553.
- 741 40. Gempe T, Beye M: Function and evolution of sex determination mechanisms, genes and
742 pathways in insects. *Bioessays* 2011, 33:52-60.
- 743 41. Nelson-Rees WA, Hoy MA, Roush RT: Heterochromatinization, chromatin elimination and
744 haploidization in the parahaploid mite *Metaseiulus occidentalis* (Nesbitt) (Acarina:
745 Phytoseiidae). *Chromosoma* 1980, 77:263-276.
- 746 42. Sutovsky P: Sperm proteasome and fertilization. *Reproduction* 2011, 142:1-14.
- 747 43. Baker ME: Evolution of 17beta-hydroxysteroid dehydrogenases and their role in androgen,
748 estrogen and retinoid action. *Mol Cell Endocrinol* 2001, 171:211-215.
- 749 44. Britton C, Murray L: Cathepsin L protease (CPL-1) is essential for yolk processing during
750 embryogenesis in *Caenorhabditis elegans*. *J Cell Sci* 2004, 117:5133-5143.
- 751 45. Mediannikov O, Sekeyová Z, Birg ML, Raoult D: A novel obligate intracellular
752 gamma-proteobacterium associated with ixodid ticks, *Diplorickettsia massiliensis*, Gen. Nov.,
753 Sp. Nov. *PLoS One* 2010, 5:e11478.
- 754 46. Chaisiri K, McGarry JW, Morand S, Makepeace BL: Symbiosis in an overlooked microcosm:
755 a systematic review of the bacterial flora of mites. *Parasitology* 2015, 142:1152-1162.
- 756 47. Dunning Hotopp JC, Clark ME, Oliveira DC, Foster JM, Fischer P, Muñoz Torres MC,
757 Giebel JD, Kumar N, Ishmael N, Wang S, et al: Widespread lateral gene transfer from
758 intracellular bacteria to multicellular eukaryotes. *Science* 2007, 317:1753-1756.
- 759 48. Leclerque A: Whole genome-based assessment of the taxonomic position of the arthropod
760 pathogenic bacterium *Rickettsiella grylli*. *FEMS Microbiol Lett* 2008, 283:117-127.
- 761 49. Yang B, Peng G, Li T, Kadowaki T: Molecular and phylogenetic characterization of honey
762 bee viruses, *Nosema* microsporidia, protozoan parasites, and parasitic mites in China.
763 *Ecology and Evolution* 2013, 3:298-311.
- 764 50. Dainat B, Ken T, Berthoud H, Neumann P: The ectoparasitic mite *Tropilaelaps mercedesae*
765 (Acari, Laelapidae) as a vector of honeybee viruses. *Insectes Sociaux* 2009, 56:40-43.
- 766 51. Forsgren E, de Miranda JR, Isaksson M, Wei S, Fries I: Deformed wing virus associated with
767 *Tropilaelaps mercedesae* infesting European honey bees (*Apis mellifera*). *Experimental and*
768 *Applied Acarology* 2009, 47:87-97.
- 769 52. Erban T, Harant K, Hubalek M, Vitamvas P, Kamler M, Poltronieri P, Tyl J, Markovic M,
770 Titera D: In-depth proteomic analysis of *Varroa destructor*: Detection of DWV-complex,

- 771 ABPV, VdMLV and honeybee proteins in the mite. *Sci Rep* 2015, 5:13907.
- 772 53. Mordecai GJ, Wilfert L, Martin SJ, Jones IM, Schroeder DC: Diversity in a honey bee
773 pathogen: first report of a third master variant of the Deformed Wing Virus quasispecies.
774 *ISME J* 2016, 10:1264-1273.
- 775 54. Martin S, Highfield A, Brettell L, Villalobos E, Budge G, Powell M, Nikaido S, Schroeder D:
776 Global Honey Bee Viral Landscape Altered by a Parasitic Mite. *Science* 2012,
777 336:1304-1306.
- 778 55. Anderson DL, Morgan MJ: Genetic and morphological variation of bee-parasitic Tropilaelaps
779 mites (Acari: Laelapidae): new and re-defined species. *Exp Appl Acarol* 2007, 43:1-24.
- 780 56. Bennett M, Leitch I, Price H, Johnston J: Comparisons with *Caenorhabditis* (similar to 100
781 Mb) and *Drosophila* (similar to 175 Mb) using flow cytometry show genome size in
782 *Arabidopsis* to be similar to 157 Mb and thus similar to 25 % larger than the *Arabidopsis*
783 genome initiative estimate of similar to 125 Mb. *Annals of Botany* 2003, 91:547-557.
- 784 57. Weinstock G, Robinson G, Gibbs R, Worley K, Evans J, Maleszka R, Robertson H, Weaver D,
785 Beye M, Bork P, et al: Insights into social insects from the genome of the honeybee *Apis*
786 *mellifera*. *Nature* 2006, 443:931-949.
- 787 58. Marcais G, Kingsford C: A fast, lock-free approach for efficient parallel counting of
788 occurrences of k-mers. *Bioinformatics* 2011, 27:764-770.
- 789 59. Zhang G, Fang X, Guo X, Li L, Luo R, Xu F, Yang P, Zhang L, Wang X, Qi H, et al: The
790 oyster genome reveals stress adaptation and complexity of shell formation. *Nature* 2012,
791 490:49-54.
- 792 60. Zerbino D, Birney E: Velvet: Algorithms for de novo short read assembly using de Bruijn
793 graphs. *Genome Research* 2008, 18:821-829.
- 794 61. Benson G: Tandem repeats finder: a program to analyze DNA sequences. *Nucleic Acids*
795 *Research* 1999, 27:573-580.
- 796 62. Trapnell C, Pachter L, Salzberg S: TopHat: discovering splice junctions with RNA-Seq.
797 *Bioinformatics* 2009, 25:1105-1111.
- 798 63. Trapnell C, Williams BA, Pertea G, Mortazavi A, Kwan G, van Baren MJ, Salzberg SL, Wold
799 BJ, Pachter L: Transcript assembly and quantification by RNA-Seq reveals unannotated
800 transcripts and isoform switching during cell differentiation. *Nat Biotechnol* 2010,
801 28:511-515.
- 802 64. Stanke M, Morgenstern B: AUGUSTUS: a web server for gene prediction in eukaryotes that
803 allows user-defined constraints. *Nucleic Acids Research* 2005, 33:W465-W467.
- 804 65. Korf I: Gene finding in novel genomes. *Bmc Bioinformatics* 2004, 5.
- 805 66. Lukashin AV, Borodovsky M: GeneMark.hmm: new solutions for gene finding. *Nucleic Acids*
806 *Res* 1998, 26:1107-1115.
- 807 67. Cantarel B, Korf I, Robb S, Parra G, Ross E, Moore B, Holt C, Alvarado A, Yandell M:
808 MAKER: An easy-to-use annotation pipeline designed for emerging model organism
809 genomes. *Genome Research* 2008, 18:188-196.
- 810 68. Zdobnov EM, Apweiler R: InterProScan--an integration platform for the
811 signature-recognition methods in InterPro. *Bioinformatics* 2001, 17:847-848.
- 812 69. Lowe TM, Eddy SR: tRNAscan-SE: a program for improved detection of transfer RNA genes

- 813 in genomic sequence. *Nucleic Acids Res* 1997, 25:955-964.
- 814 70. Nawrocki EP, Eddy SR: Infernal 1.1: 100-fold faster RNA homology searches.
815 *Bioinformatics* 2013, 29:2933-2935.
- 816 71. Conesa A, Götz S, García-Gómez JM, Terol J, Talón M, Robles M: Blast2GO: a universal
817 tool for annotation, visualization and analysis in functional genomics research.
818 *Bioinformatics* 2005, 21:3674-3676.
- 819 72. Kanehisa M, Goto S: KEGG: kyoto encyclopedia of genes and genomes. *Nucleic Acids Res*
820 2000, 28:27-30.
- 821 73. Katoh K, Standley DM: MAFFT multiple sequence alignment software version 7:
822 improvements in performance and usability. *Mol Biol Evol* 2013, 30:772-780.
- 823 74. Lassmann T, Frings O, Sonnhammer EL: Kalign2: high-performance multiple alignment of
824 protein and nucleotide sequences allowing external features. *Nucleic Acids Res* 2009,
825 37:858-865.
- 826 75. Castresana J: Selection of conserved blocks from multiple alignments for their use in
827 phylogenetic analysis. *Mol Biol Evol* 2000, 17:540-552.
- 828 76. Darriba D, Taboada GL, Doallo R, Posada D: ProtTest 3: fast selection of best-fit models of
829 protein evolution. *Bioinformatics* 2011, 27:1164-1165.
- 830 77. Guindon S, Dufayard JF, Lefort V, Anisimova M, Hordijk W, Gascuel O: New algorithms and
831 methods to estimate maximum-likelihood phylogenies: assessing the performance of PhyML
832 3.0. *Syst Biol* 2010, 59:307-321.
- 833 78. Ronquist F, Huelsenbeck JP: MrBayes 3: Bayesian phylogenetic inference under mixed
834 models. *Bioinformatics* 2003, 19:1572-1574.
- 835 79. Tamura K, Stecher G, Peterson D, Filipski A, Kumar S: MEGA6: Molecular Evolutionary
836 Genetics Analysis version 6.0. *Mol Biol Evol* 2013, 30:2725-2729.
- 837 80. Adams M, Celniker S, Holt R, Evans C, Gocayne J, Amanatides P, Scherer S, Li P, Hoskins
838 R, Galle R, et al: The genome sequence of *Drosophila melanogaster*. *Science* 2000,
839 287:2185-2195.
- 840 81. Sanggaard KW, Bechsgaard JS, Fang X, Duan J, Dyrland TF, Gupta V, Jiang X, Cheng L,
841 Fan D, Feng Y, et al: Spider genomes provide insight into composition and evolution of
842 venom and silk. *Nat Commun* 2014, 5:3765.
- 843 82. Stein L, Sternberg P, Durbin R, Thierry-Mieg J, Spieth J: WormBase: network access to the
844 genome and biology of *Caenorhabditis elegans*. *Nucleic Acids Research* 2001, 29:82-86.
- 845 83. Dabert M, Witalinski W, Kazmierski A, Olszanowski Z, Dabert J: Molecular phylogeny of
846 acariform mites (Acari, Arachnida): strong conflict between phylogenetic signal and
847 long-branch attraction artifacts. *Mol Phylogenet Evol* 2010, 56:222-241.
- 848 84. Yang Z: PAML 4: phylogenetic analysis by maximum likelihood. *Mol Biol Evol* 2007,
849 24:1586-1591.
- 850 85. Li L, Stoeckert CJ, Roos DS: OrthoMCL: identification of ortholog groups for eukaryotic
851 genomes. *Genome Res* 2003, 13:2178-2189.
- 852 86. De Bie T, Cristianini N, Demuth JP, Hahn MW: CAFE: a computational tool for the study of
853 gene family evolution. *Bioinformatics* 2006, 22:1269-1271.
- 854 87. Anders S, Pyl PT, Huber W: HTSeq—a Python framework to work with high-throughput

855 sequencing data. *Bioinformatics* 2015, 31:166-169.

856 88. Robinson MD, McCarthy DJ, Smyth GK: edgeR: a Bioconductor package for differential
857 expression analysis of digital gene expression data. *Bioinformatics* 2010, 26:139-140.

858 89. Bourgon R, Gentleman R, Huber W: Independent filtering increases detection power for
859 high-throughput experiments. *Proc Natl Acad Sci U S A* 2010, 107:9546-9551.

860 90. Dimont E, Shi J, Kirchner R, Hide W: edgeRun: an R package for sensitive, functionally
861 relevant differential expression discovery using an unconditional exact test. *Bioinformatics*
862 2015, 31:2589-2590.

863 91. Elsik CG, Worley KC, Bennett AK, Beye M, Camara F, Childers CP, de Graaf DC, Debyser
864 G, Deng J, Devreese B, et al: Finding the missing honey bee genes: lessons learned from a
865 genome upgrade. *BMC Genomics* 2014, 15:86.

866 92. Vizcaíno JA, Csordas A, del-Toro N, Dianes JA, Griss J, Lavidas I, Mayer G, Perez-Riverol
867 Y, Reisinger F, Ternent T, et al: 2016 update of the PRIDE database and its related tools.
868 *Nucleic Acids Res* 2016, 44:D447-456.

869 93. Sánchez - Gracia A, Vieira FG, Almeida FC, Rozas J: Comparative genomics of the major
870 chemosensory gene families in Arthropods. *eLS* 2011.

871 94. Feyereisen R, Lawrence I: 8-insect CYP genes and P450 enzymes. *Insect molecular biology
872 and biochemistry* 2012:236-316.

875 Table 1 Genome statistics for *T. mercedesae*

| | | |
|----|--------------------------------|---------|
| 1 | Estimated genome size (Mb) | 660 |
| 2 | Assembled genome Size (Mb) | 353 |
| 3 | GC content (%) | 44 |
| 4 | Total scaffold number | 34,155 |
| 5 | Largest scaffold (kb) | 327,111 |
| 6 | N50 size (bp) | 28,807 |
| 7 | Complete CEGs (%) | 91.94 |
| 8 | Partial CEGs (%) | 98.39 |
| 9 | Number of protein-coding genes | 15,190 |
| 10 | Average exon length (bp) | 363 |
| 11 | Average intron length (bp) | 820 |

12

13

14

15

16

17

18

19

20

21

22

23

24

25

26

27

28

29

30

31

32

33

34

35

36

37

38

39

40

41

42

43

44

45

46

47

48

49

876
877
878 Table 2 The number of genes associated with chemosensory system in *T. mercedesae* and other
879 arthropods.

| Species | GR | OR | IR | OBP | CSP |
|------------------------|----|-----|----|-----|-----|
| <i>T. mercedesae</i> | 5 | 0 | 8 | 0 | 0 |
| <i>M. occidentalis</i> | 64 | 0 | 65 | 0 | 0 |
| <i>I. scapularis</i> | 60 | 0 | 22 | 0 | 1 |
| <i>S. maritima</i> | 77 | 0 | 60 | 0 | 2 |
| <i>D. pulex</i> | 53 | 0 | 85 | 0 | 3 |
| <i>D. melanogaster</i> | 73 | 62 | 66 | 51 | 4 |
| <i>A. mellifera</i> | 10 | 163 | 10 | 21 | 6 |
| <i>B. mori</i> | 56 | 48 | 18 | 44 | 18 |
| <i>A. pisum</i> | 53 | 48 | 11 | 15 | 13 |
| <i>P. humanus</i> | 8 | 10 | 12 | 5 | 7 |

880 The numbers of GR (gustatory receptor), OR (olfactory receptor), IR (ionotropic receptor), OBP
881 (olfactory binding protein), and CSP (chemosensory protein) genes in *T. mercedesae* and nine
882 arthropod species including *Bombyx mori* and *Acyrtosiphon pisum* are shown. Data referred to
883 references [16, 31, 93] and this study.

884

885

886

887

888

889

890

891

892

893

894

895

896

897

898

899

900

885 Table 3 Comparison of the number of CYP2, 3, 4, and mitochondrial clan members in Insecta,
 886 Crustacea, and Acari.

| | Total | CYP2 | CYP3 | CYP4 | Mitochondria |
|------------------------|---------|---------|---------|------|--------------|
| Insecta | | | | | |
| <i>D. melanogaster</i> | 88 | 7 | 11 | 32 | 36 |
| <i>A. gambiae</i> | 105 | 10 | 9 | 46 | 40 |
| <i>A. aegypti</i> | 160 | 12 | 9 | 57 | 82 |
| <i>B. mori</i> | 85 | 7 | 12 | 36 | 30 |
| <i>A. mellifera</i> | 46 | 8 | 6 | 4 | 28 |
| <i>N. vitripennis</i> | 92 | 7 | 7 | 30 | 48 |
| <i>T. castaneum</i> | 134 | 8 | 9 | 45 | 72 |
| <i>A. pisum</i> | 64 | 10 | 8 | 23 | 23 |
| <i>P. humanus</i> | 36 | 8 | 8 | 9 | 11 |
| Crustacea | | | | | |
| <i>D. pulex</i> | 75 | 20 | 6 | 37 | 12 |
| Acari | | | | | |
| <i>T. mercedesae</i> | 56 | 7 | 19 | 20 | 10 |
| <i>M. occidentalis</i> | 75 (63) | 19 (16) | 32 (23) | 19 | 5 |
| <i>T. urticae</i> | 86 | 48 | 5 | 23 | 10 |

887 The data of four insects, *Anopheles gambiae*, *Aedes aegypti*, *Nasonia vitripennis*, and *Tribolium*
 888 *castaneum* are also included. Data referred to references [94] and this study. The numbers in
 889 parentheses are derived from previous report [37].

891 **Figure legends**

892

893 **Figure 1 Comparative genomics.**

894 (A) The species phylogeny was built from aligned protein sequences of 926 one-to-one orthologs in
895 *Metaseiulus occidentalis*, *Tropilaelaps mercedesae*, *Ixodes scapularis*, *Stegodyphus mimosarum*,
896 *Tetranychus urticae*, *Drosophila melanogaster*, and *Apis mellifera* using a maximum likelihood
897 method. The tree was rooted with *Caenorhabditis elegans*. All nodes showed 100% bootstrap
898 support. Protein-coding genes were classified into the different categories. 1:1:1 orthologs and
899 N:N:N orthologs represent the common orthologs with the same copy numbers and different copy
900 numbers, respectively. Patchy orthologs are shared between more than one but not all species
901 (excluding those in the previous categories). Unclustered genes represent genes classified to
902 unknown gene families. Other categories include arthropod-, Arachnida-, Parasitiformes-, and
903 species-specific genes. *C. elegans* was used as the outgroup for classification of the protein-coding
904 genes. (B) The number of gene families shared between *T. mercedesae*, *M. occidentalis*, *I. scapularis*,
905 and other reference species (*S. mimosarum*, *T. urticae*, *D. melanogaster*, and *A. mellifera*) by
906 Orthomcl classification algorithm.

907

908 **Figure 2 Phylogenetic tree of *T. mercedesae*, *I. scapularis*, and *D. melanogaster* gustatory
909 receptors.**

910 Phylogenetic tree of *T. mercedesae* (red), *I. scapularis* (blue), and *D. melanogaster* (green) gustatory
911 receptors (GRs) was constructed by a maximum likelihood method. Two clusters of fruit fly GRs
912 responding to sugar and CO₂ are indicated. The tree was rooted at the middle point.

913

914 **Figure 3 Phylogeny of *T. mercedesae*, *M. occidentalis*, and *D. melanogaster* cytochrome P450.**

915 The phylogenetic tree was constructed by maximum likelihood method and rooted at the middle
916 point. P450s are clustered to CYP2, CYP3, CYP4, and mitochondrial clans are shown by red, green,
917 blue, and dark yellow branches, respectively. *D. melanogaster* (DmCYP), *T. mercedesae*, and *M.*
918 *occidentalis* P450s are indicated by dark green, purple, and dark yellow, respectively. *T. mercedesae*
919 and *M. occidentalis* P450s are designated by protein IDs.

920

921 **Figure 4 Volcano plot of proteins in the male and female mites.**

922 Proteins identified in the male and female mites by proteomic analysis are plotted according to the
923 ratios of amounts present in male to female. Proteins abundant in the male and female are indicated
924 by blue and red circles, respectively. Some of the representative proteins are indicated with the
925 names and accession numbers of the best Blast hits.

926

927 **Figure 5 %GC-coverage plots of the preliminary assembled genomes of male and female.**

928 Individual contigs are plotted based on their GC content (x-axis) and their node coverage (y-axis;
929 logarithmic scale). Contigs are colored according to the taxonomic order of their best Megablast hit
930 to the NCBI nr database (with E-value cut off < 1e-5). Contigs without the annotation are in gray. %
931 GC plots against node coverage for the (A) male and (B) female contigs are shown in.

932

60

61

62

63

64

65

933 **Figure 6 Classification of DWV in the *T. mercedesae* transcriptomes.**

934 The Bayesian phylogeny was constructed using Mrbayers based on the amino acid sequences of
935 complete DWV genomes assembled from the adult males, adult females and nymphs transcriptomes
936 (DWV weixi strain complete genome male, DWV weixi strain complete genome female, and DWV
937 weixi strain complete genome nymph) as well as seven other DWV strains (type A variant:
938 NC_005876.1, NC_004830.2, JQ_413340, and ERS657948; type B: KC_786222.1 and
939 NC_006494.1; type C: ERS657949). The tree was rooted with Formica exsecta Virus 1
940 (NC_023022.1) and Sacbrood Virus (NC_002066.1).

941
12
13
14
15
16
17
18
19
20
21
22
23
24
25
26
27
28
29
30
31
32
33
34
35
36
37
38
39
40
41
42
43
44
45
46
47
48
49
50
51
52
53
54
55
56
57
58
59
60
61
62
63
64
65

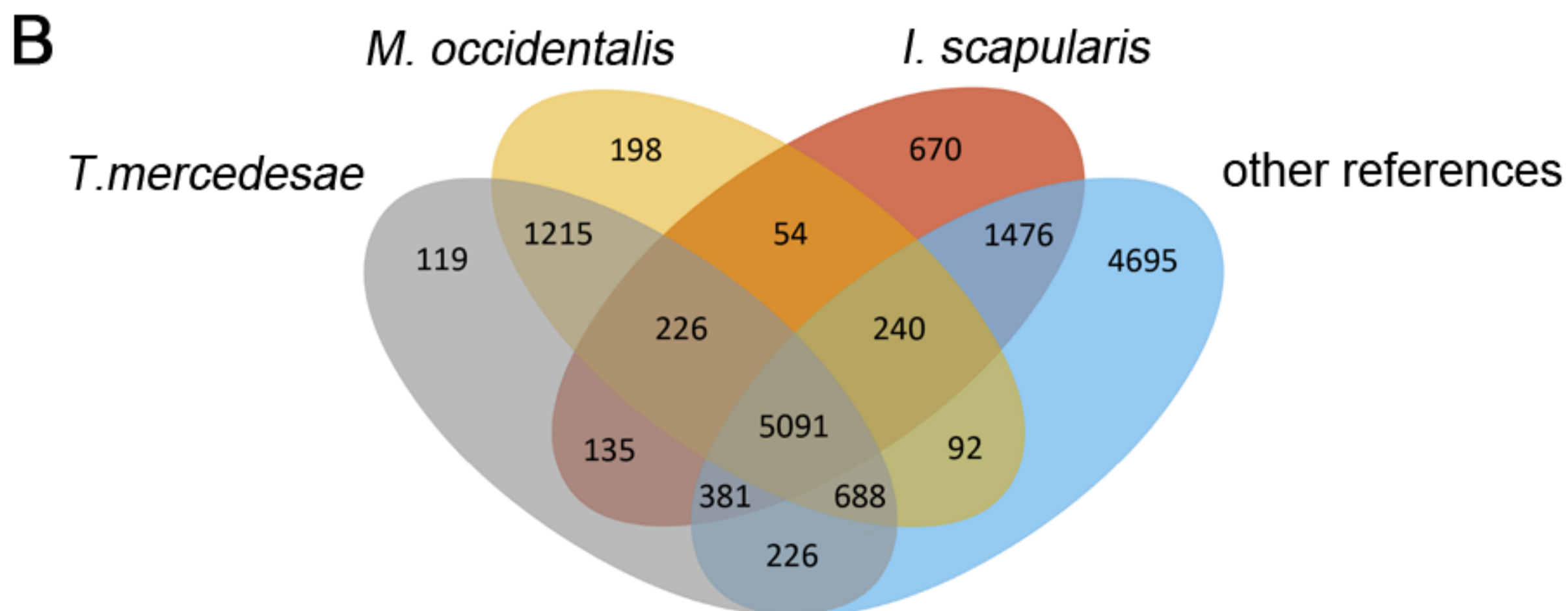
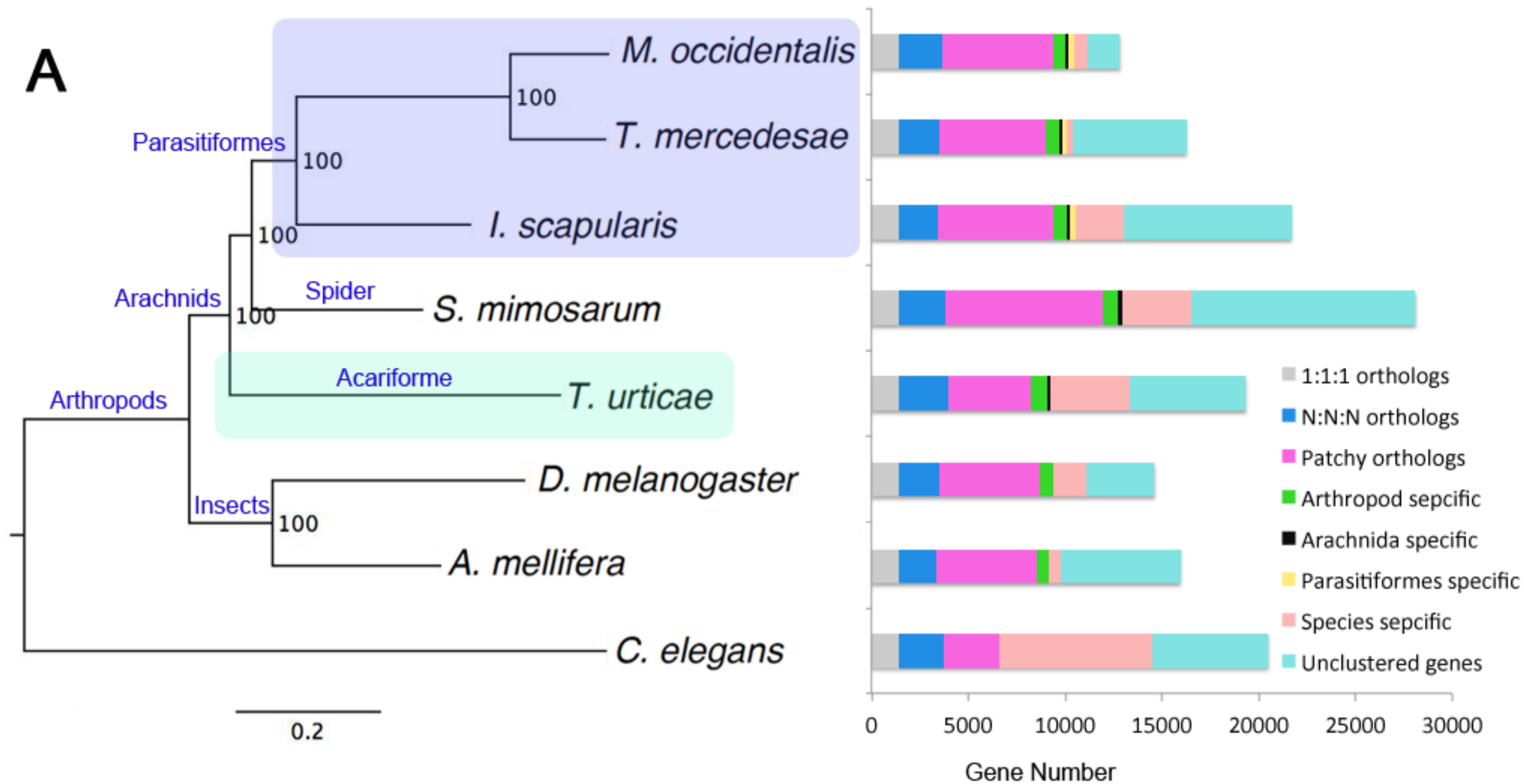
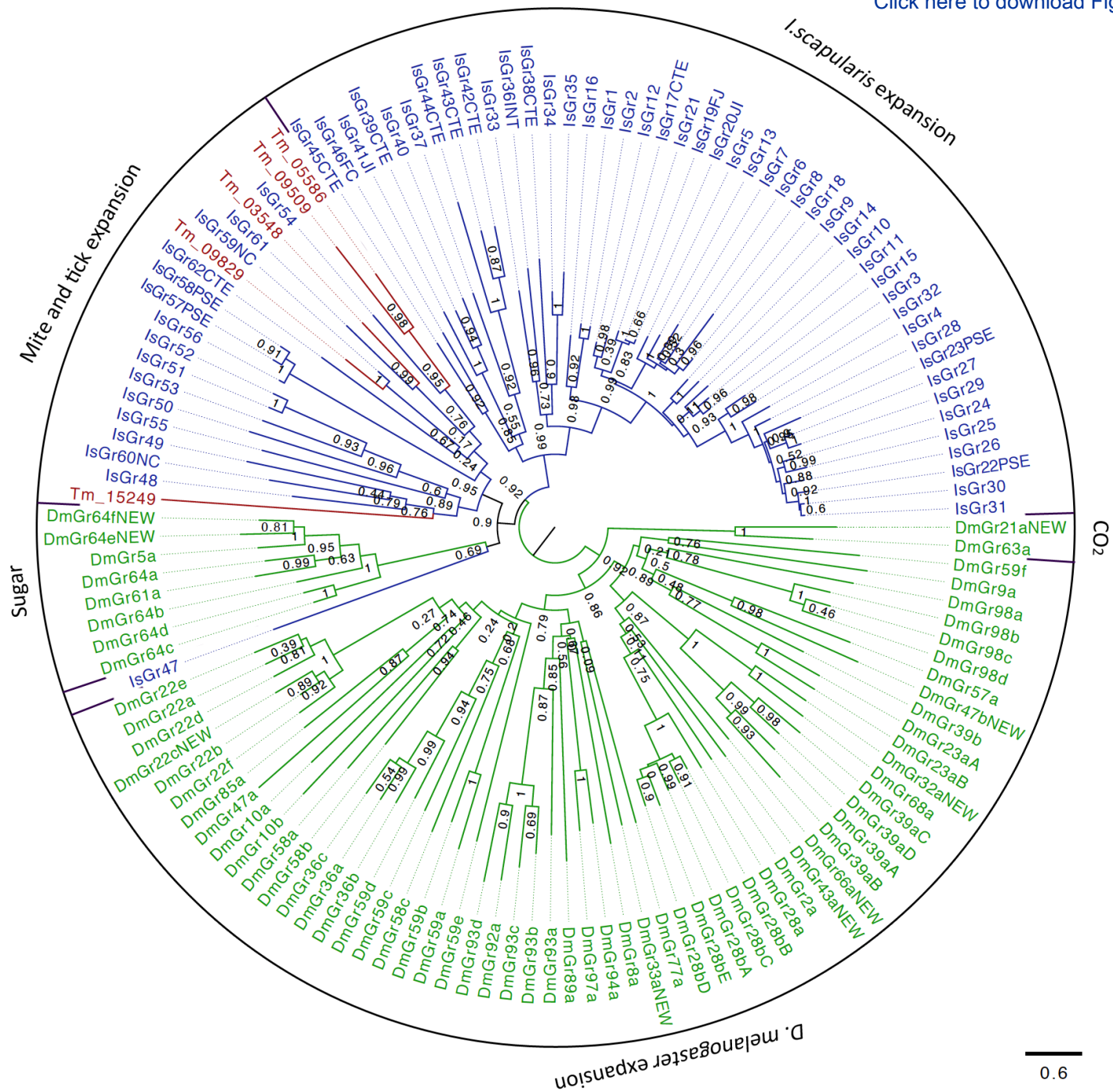
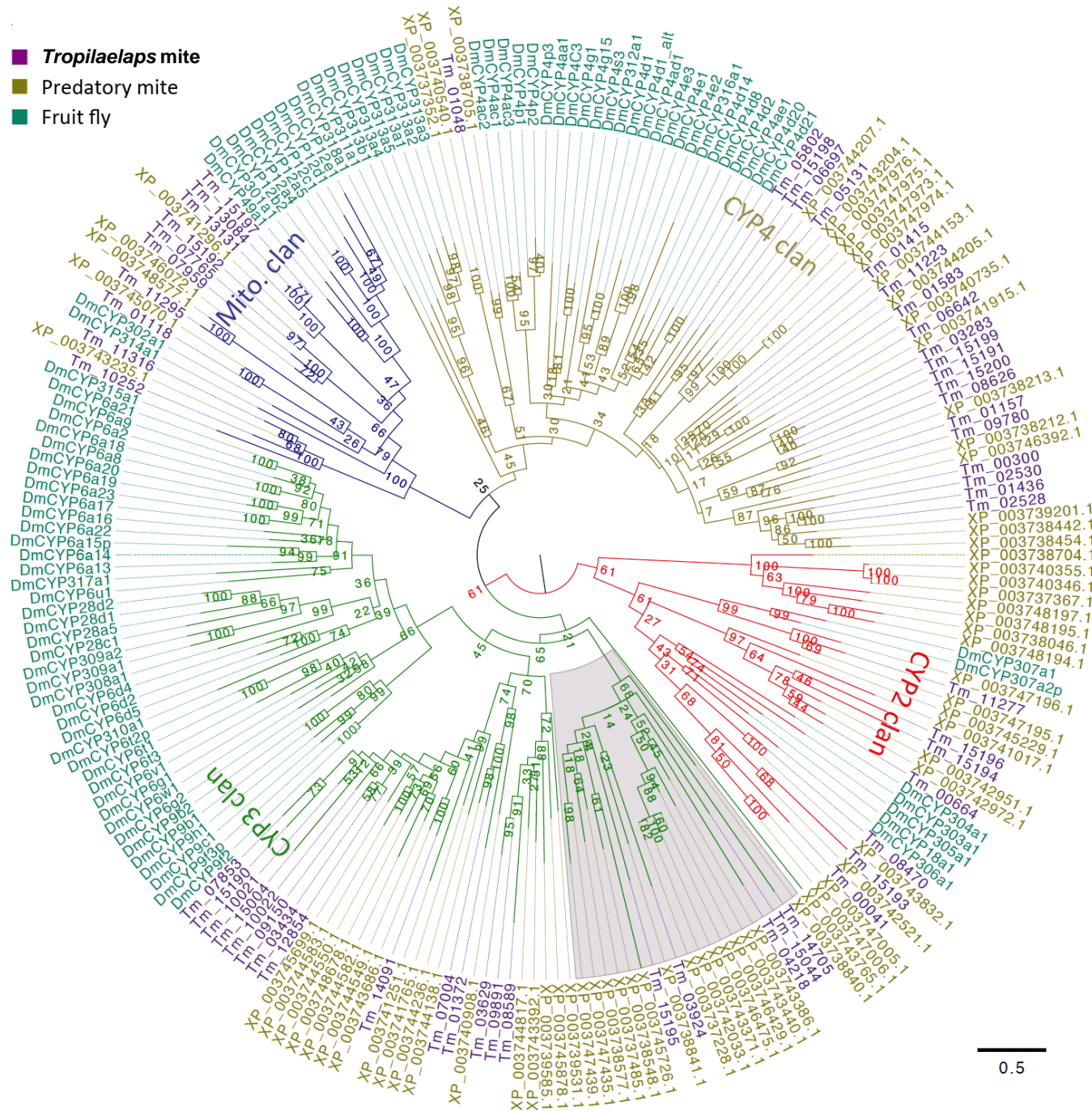


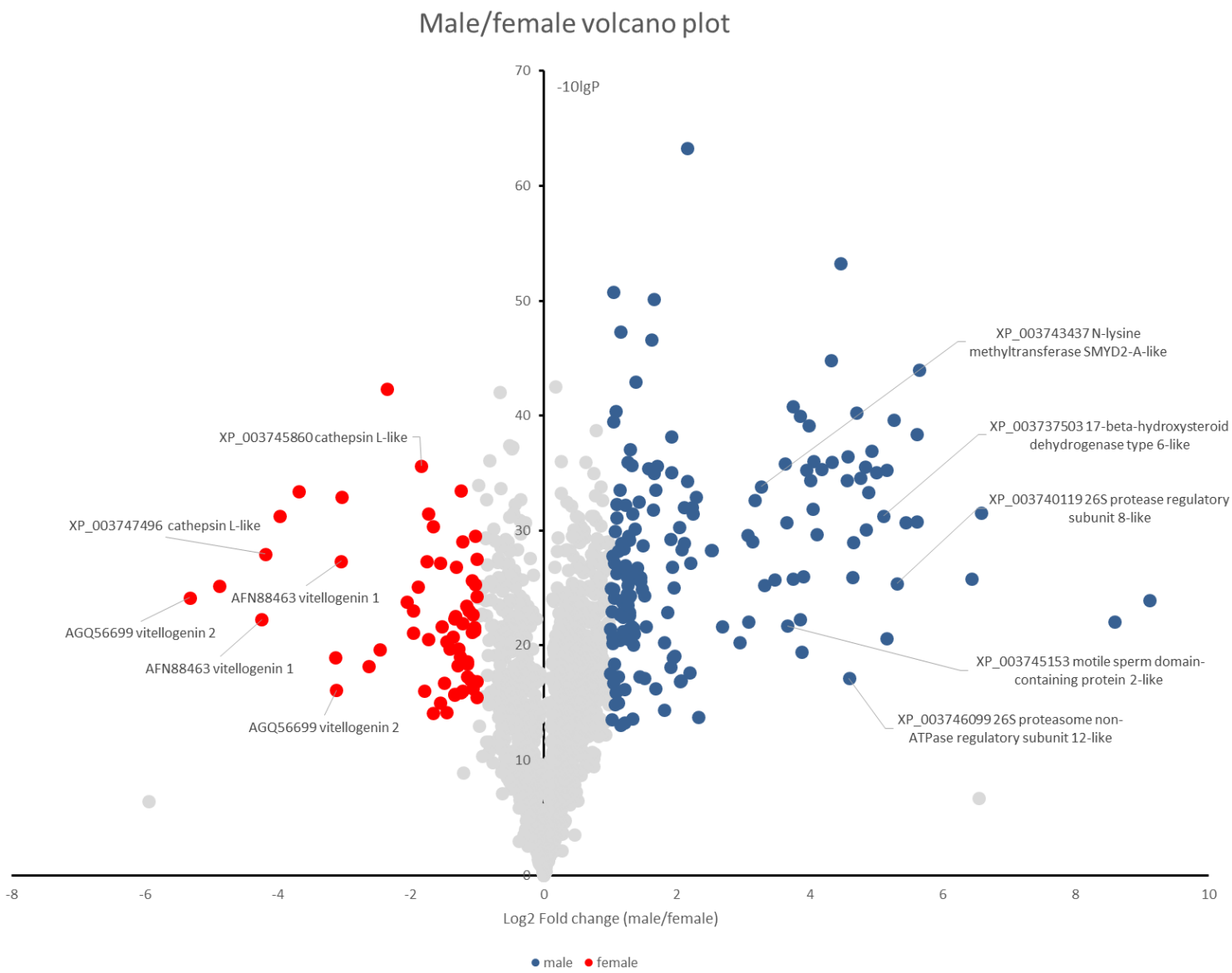
Figure 2

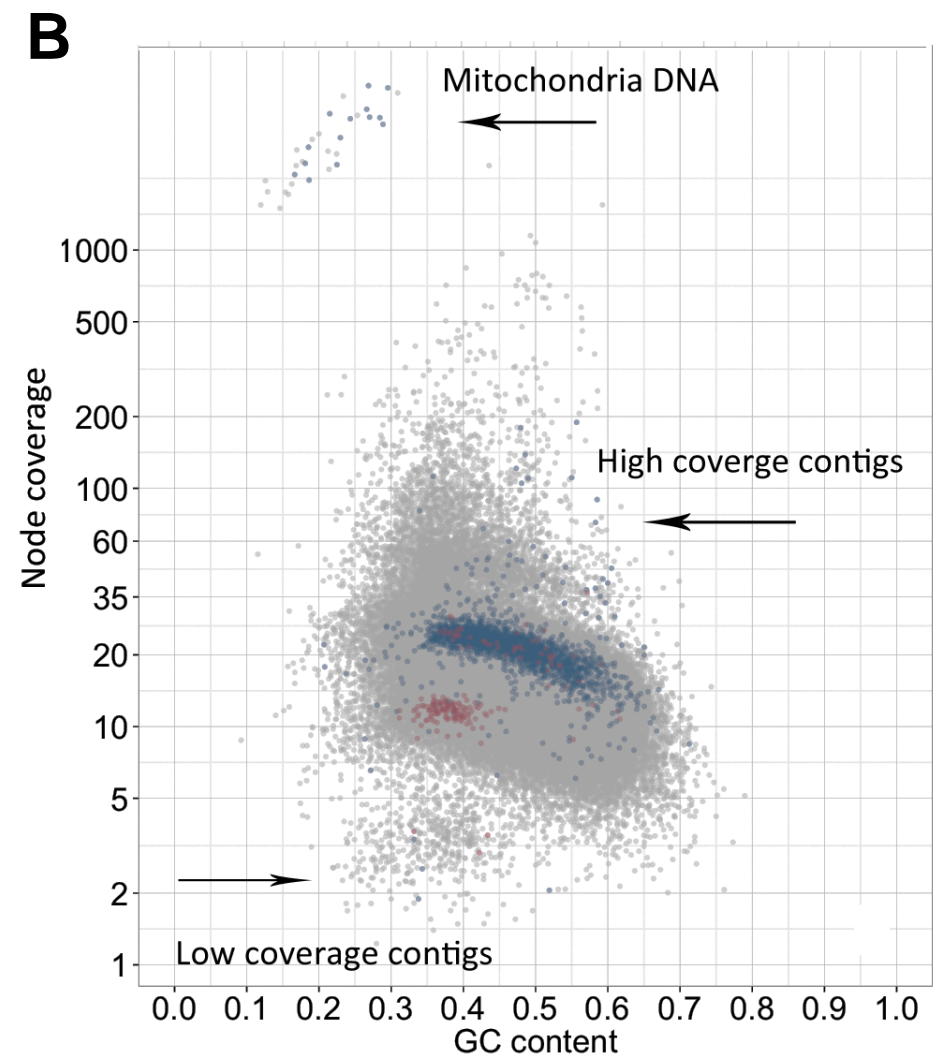
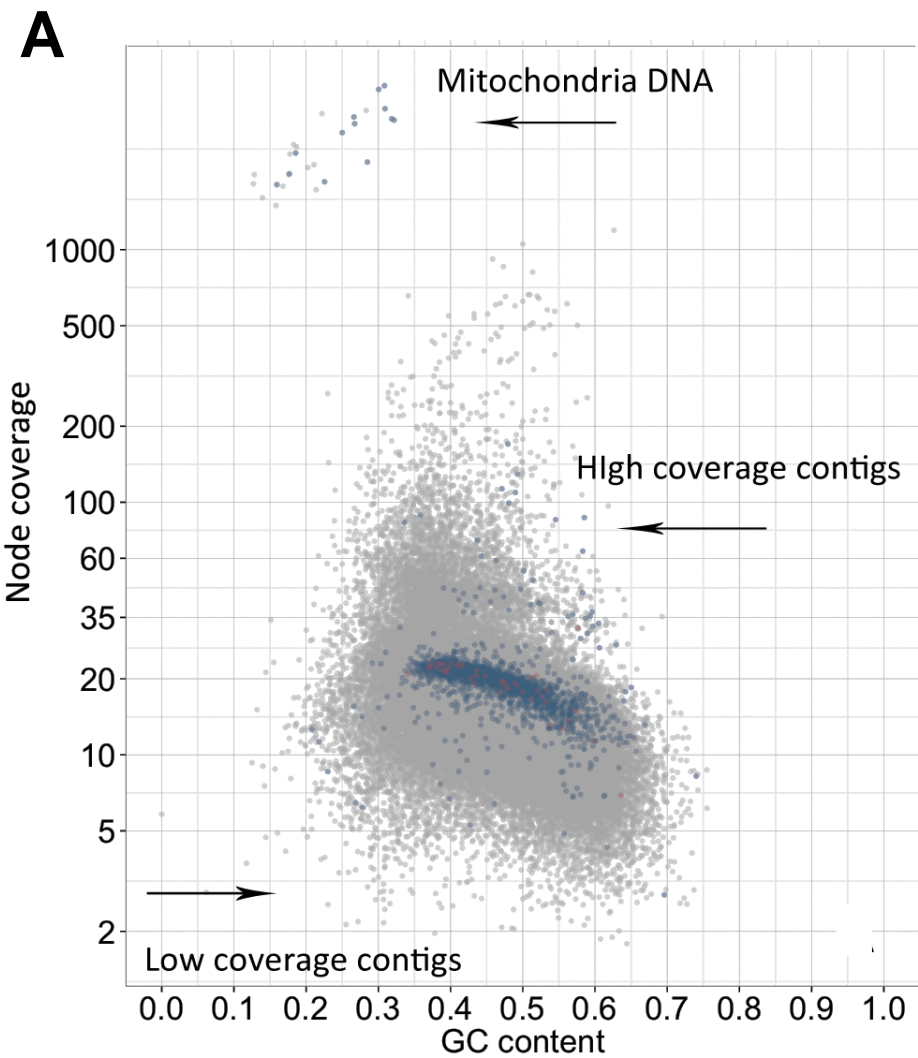


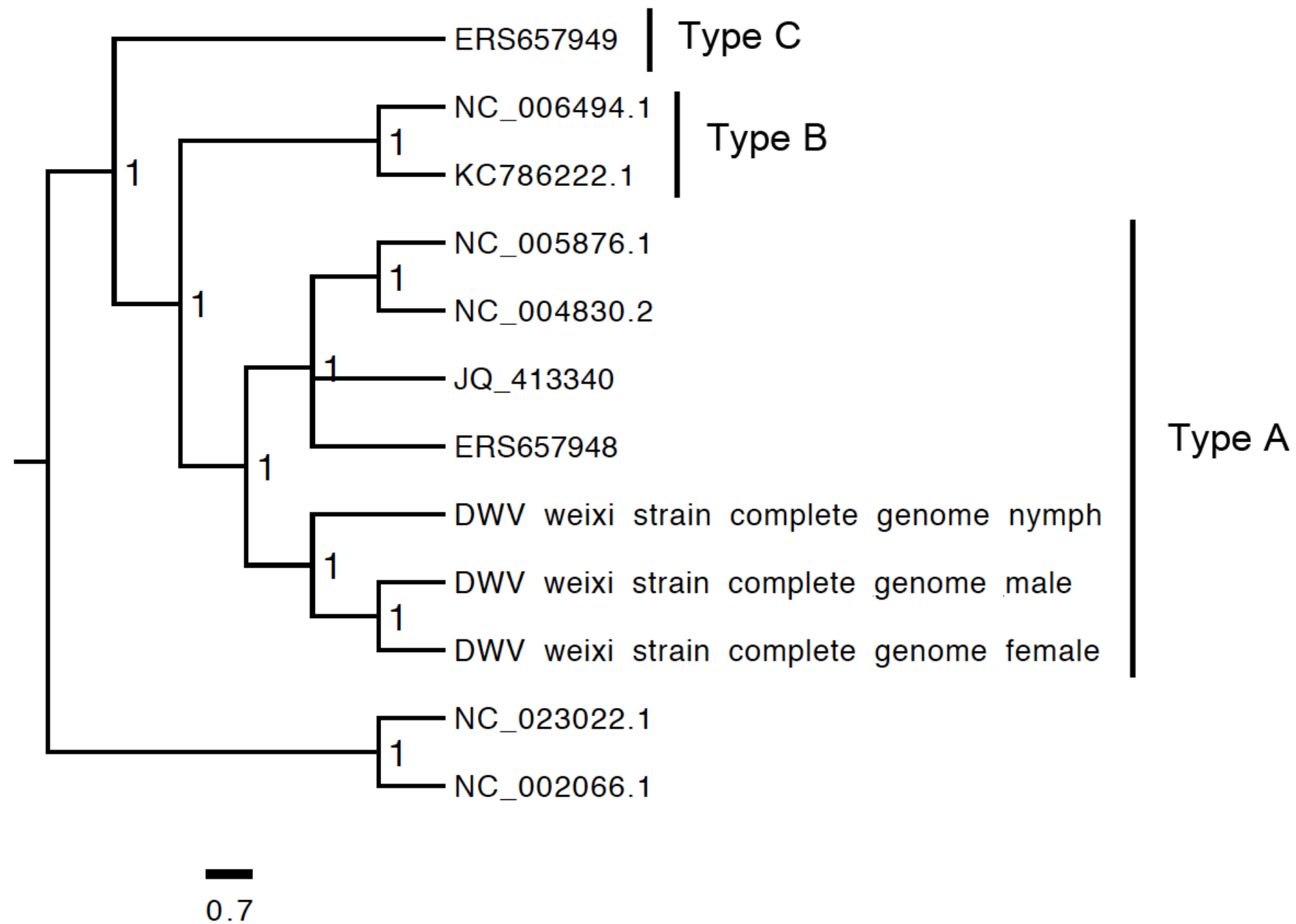
0.6

- *Tropilaelaps* mite
- Predatory mite
- Fruit fly











Click here to access/download
Supplementary Material
Supplementary file 1.xlsx





Click here to access/download
Supplementary Material
Dong et al_Supplementary Tables.doc





Click here to access/download
Supplementary Material
Dong et al_Supplementary Figures.doc

